

1 Carbon dynamics at the river-estuarine transition: a comparison among tributaries
2 of Chesapeake Bay.

3 Paul A. Bukaveckas

4 Center for Environmental Studies
5 Virginia Commonwealth University
6 Richmond, Virginia, USA

7
8 Submitted to: Biogeosciences

9 August 3, 2021

10 revised December 17, 2021

11 Corresponding author: Paul Bukaveckas (pabukaveckas@vcu.edu)

12 Keywords: carbon, estuaries, mass balance CO₂ flux

13

14 **Abstract**

15 Sources and transformation of C were quantified using mass balance and ecosystem metabolism
16 data for the upper segments of the James, Pamunkey and Mattaponi Estuaries. The goal was to
17 assess the role of external (river inputs & tidal exchange) vs. internal (metabolism) drivers in
18 influencing the forms and fluxes of C. C forms and their response to river discharge differed
19 among the estuaries based on their physiographic setting. The James, which receives the bulk of
20 inputs from upland areas (Piedmont and Mountain), exhibited a higher ratio of inorganic to
21 organic C, and larger inputs of POC. The Pamunkey and Mattaponi receive a greater proportion
22 of inputs from lowland (Coastal Plain) areas, which were characterized by low DIC and POC,
23 and elevated DOC. I anticipated that transport processes would dominate during colder months
24 when discharge is elevated and metabolism is low, and that biological processes would
25 predominate in summer, leading to attenuation of C through-puts via de-gassing of CO₂.
26 Contrary to expectations, highest retention of OC occurred during periods of high through-put, as
27 elevated discharge resulted in greater loading and retention of POC. In summer, internal cycling
28 of C via production and respiration was large in comparison to external forcing despite the large
29 riverine influence in these upper estuarine segments. The estuaries were found to be net
30 heterotrophic based on retention of OC, export of DIC, low GPP relative to ER, and a net flux of
31 CO₂ to the atmosphere. In the James, greater contributions from phytoplankton production
32 resulted in a closer balance between GPP and ER, with autochthonous production exceeding
33 allochthonous inputs. Combining the mass balance and metabolism data with bioenergetics
34 provided a basis for estimating the proportion of C inputs utilized by the dominant metazoan.
35 The findings suggest that invasive catfish utilize 15% of total OM inputs and up to 40% of
36 allochthonous inputs to the James.

37 Non-technical summary: Inland waters play an important role in the global carbon cycle by
38 storing, transforming and transporting carbon from land to sea. Comparatively little is known
39 about carbon dynamics at the river-estuarine transition. A study of tributaries of Chesapeake
40 Bay showed that biological processes exerted a strong effect on carbon transformations. Peak
41 carbon retention occurred during periods of elevated river discharge and was associated with
42 trapping of particulate matter.

43 **1. Introduction**

44 Inland waters occupy a small proportion of surface area but play a disproportionately large role
45 in global C cycling (Cole et al. 2007; Butman et al. 2016; Tranvik et al. 2018; Holgerson and
46 Raymond 2016). River networks act as transport systems delivering C products of mineral
47 weathering (DIC) and plant decomposition (DOC, POC) from the terrestrial realm to the coastal
48 ocean (Meybeck 2003). Inland waters also function as reactors in which biotic and abiotic
49 processes act to augment, transform or attenuate C fluxes. Aquatic primary production
50 supplements terrestrial DOC and POC inputs, and by providing more labile forms of C, may
51 facilitate the decomposition of older, recalcitrant terrestrial C. Decomposition of aquatic and
52 terrestrial organic matter returns C to the atmosphere, which, along with C sequestration via
53 sediment burial, results in the attenuation of C fluxes to the coastal zone (Richey et al. 2002;
54 Vorosmarty et al. 2003; Middelburg and Herman 2007; Tranvik et al. 2009). Acting against
55 these processes are fluvial forces that hasten through-puts of C and favor transport over
56 processing. Along the flowpath from mountains to the sea, aquatic systems differ greatly in their
57 capacity to attenuate C fluxes depending on factors such as water residence time, ecosystem
58 metabolism and capacity for sediment accrual. Biological processes are expected to exert a
59 stronger influence over C transport in lakes relative to streams and rivers, owing to their longer
60 water residence time (Hotchkiss et al. 2018). Current efforts focus on understanding the net
61 effect of inland waters on landscape scale fluxes of C. In this context, comparatively little
62 attention has been focused on processes occurring at the river-estuarine transition.

63 The river-estuarine ecotone is defined by the transition from fluvial- to tidal-dominated forces,
64 which results in a shift from unidirectional to bidirectional flow. In some settings, the point of
65 transition may migrate in response to changing discharge conditions, with fluvial forces
66 extending seaward during high discharge, and tidal forces gaining inland during periods of low
67 freshwater inputs. Along the mid-Atlantic coast, the landward extent of tidal influence is
68 delineated by a geologic feature (the Fall Line), a zone of rapid elevation change at the transition
69 from upland (Piedmont) to lowland (Coastal Plain) physiographic regions. Below the Fall Line,
70 hydrodynamics are estuarine in that they are subject to bi-directional flows associated with
71 incoming and outgoing tides, whereas chemistry is riverine (freshwater). These conditions arise

72 because tidal forces propagate inland beyond the point where mixing of fresh and marine waters
73 occurs.

74 Tidal freshwaters are a common feature of river-dominated estuaries throughout the world but
75 have received relatively little attention in landscape-scale assessments of biogeochemical
76 processes (Hoitink and Jay 2016; Ward et al. 2017; Jones et al. 2020). A key feature of tidal
77 freshwaters is their prolonged residence time relative to non-tidal rivers (Jones et al. 2017).
78 Water and materials exported during an out-going tide are returned on the incoming tide, thereby
79 increasing residence time. For example, plankton community development in rivers is often
80 constrained by short transit time (Soballe and Kimmel 1987; Pace et al. 1992; Basu and Pick
81 1996; Sellers and Bukaveckas 2003; Lucas et al. 2009), whereas the back and forth of tidal flows
82 reduces net seaward movement resulting in longer transit time (Shen and Lin 2006; Qin and
83 Shen 2017). Bi-directional flows in tidal freshwaters create more favorable water residence time
84 conditions (relative to non-tidal rivers) that allow for the development of phytoplankton
85 communities and the potential for greater biological influence on C forms and retention. Our
86 prior work in the James Estuary has documented higher rates of ecosystem metabolism in the
87 tidal freshwater segment relative to adjacent riverine and lower estuarine segments (Tassone and
88 Bukaveckas 2019; Bukaveckas et al. 2020). The occurrence of a chlorophyll-a and productivity
89 maxima in the tidal fresh zone was attributed to longer water residence time and proximal
90 nutrient inputs from riverine and local point sources (Bukaveckas et al. 2011; Qin and Shen
91 2017). Other studies have also documented tidal freshwaters as potential biogeochemical
92 hotspots (Vincent et al. 1996; Muylaert et al. 2005; Hoffman et al. 2008; Lionard et al. 2008;
93 Amann et al. 2015; Young et al. 2021; Xu et al. 2021).

94 The goal of this study was to assess the relative importance of external (river inputs & tidal
95 exchange) vs. internal (metabolism) drivers in influencing C forms and retention in the upper
96 estuary. Long water residence time and high rates of ecosystem metabolism in the tidal fresh
97 zone were expected to favor the importance of internal processes over external hydrologic forces
98 in regulating C throughputs. During periods of low river discharge, longer water residence in the
99 estuary allows accrual of phytoplankton biomass and greater GPP, which may result in net
100 autotrophy and greater export of organic C relative to DIC. Alternatively, the production of
101 autochthonous labile C may facilitate mineralization of allochthonous C inputs (“priming

102 effect”) resulting in CO₂ release and attenuation of organic and total C exports (Bianchi 2011;
103 Steen et al. 2015; Ward et al. 2016). During periods of elevated discharge, freshwater
104 replacement time in the upper estuary is short, thereby favoring transport over retention.
105 However, our recent work has shown that the bulk of N and P retention in the tidal fresh zone of
106 the James Estuary occurs during periods of high sediment loading (Bukaveckas et al. 2018).
107 Although retention of dissolved N and P was highest during peak production in summer, the
108 trapping of particulate N and P in winter accounted for the bulk of total N and P retention. These
109 findings suggest that retention of particulate and total C may be highest during periods of
110 elevated river discharge.

111 In this study, mass balance results and ecosystem metabolism data were used to assess C inputs,
112 outputs, transformation and retention in the upper estuarine segments of two Chesapeake Bay
113 tributaries. For the James Estuary, these data are also used to estimate allochthonous and
114 autochthonous inputs and to assess constraints on food web energetics.

115

116 **2. Methods**

117 2.1 Study Sites. This study focuses on the upper segments of the two southern tributaries of
118 Chesapeake Bay (James and York Estuaries), the latter of which is comprised of two sub-
119 estuaries (Pamunkey and Mattaponi). This is the third in a series of papers that rely in part on
120 comparisons among these estuaries to draw inferences about processes occurring at the river-
121 estuarine transition. Previous papers focused on the influence of storm events on river and
122 estuarine metabolism and water quality (Bukaveckas et al. 2020), and on factors regulating water
123 clarity and primary production (Henderson & Bukaveckas 2021). The proximity of the estuaries
124 facilitated frequent sampling (1-2 week intervals) that is needed to characterize C fluxes. The
125 study reach within the James Estuary is the tidal fresh segment, which extends 88 km from the
126 Fall Line (Richmond, VA) to the confluence with the Chickahominy River, and accounts for
127 ~50% of the length of the estuary. Study reaches for the Pamunkey and Mattaponi Estuaries
128 encompassed the tidal fresh and oligohaline segments, extending 86 km to their confluence with
129 the York Estuary. A key difference among the estuaries is their geographic setting across
130 lowland (Coastal Plain) and upland (Piedmont and Mountain) areas (Figure 1). Freshwater
131 inputs to the James tidal fresh segment are largely (90%) derived from upland sources (i.e.,

132 above the Fall Line), whereas local (Coastal Plain) tributaries contribute ~10% (based on the
133 proportion of contributing area below the Fall Line). By contrast the Pamunkey and Mattaponi
134 Estuaries receive a greater proportion of freshwater inputs from local (Coastal Plain) sources
135 (36% and 51%, respectively). Higher sediment yield from upland sources should result in
136 greater POC inputs to the James relative to the Pamunkey and the Mattaponi. I also expected
137 that higher GPP and R in the phytoplankton-dominated James Estuary would exert a stronger
138 influence on C transformations relative to the Pamunkey and Mattaponi, which are dominated by
139 submerged and emergent aquatic vegetation. Lastly, extensive floodplain and wetland areas
140 along the Pamunkey and Mattaponi would be expected to contribute greater DOC inputs relative
141 to the James.

142 2.2 Data Collection. For the James, I am able to present a relatively complete C budget inclusive
143 of Fall Line loads, local tributary inputs and tidal fluxes of inorganic and organic fractions (DIC,
144 DOC, POC). These results are based on data collected from river and estuarine stations over a
145 10-year span (2010-2019). For the Pamunkey and Mattaponi, the scope is more limited both in
146 the time span over which data were collected (2017-2019) and, due to the lack of data on Fall
147 Line DIC and chloride inputs, which precludes estimation of tidal exchange using Cl mass
148 balance. For the James and Pamunkey, previously published estimates of GPP and ER derived
149 from in situ diel oxygen cycles are used to assess their effect on C transformations. Seasonal
150 patterns in CO₂ concentrations and air-water exchange are provided for all three estuaries.

151 2.3 C Inputs & Estuarine Export. External C loads for the three estuaries were derived from (a)
152 measured discharge and concentration at the Fall Line, and (b) estimated contributions from
153 ungauged tributaries below the Fall Line. Fall Line loads were based on data collected by the
154 USGS at gauging stations located on the James, Pamunkey and Mattaponi Rivers. Fall Line
155 samples were collected at approximately monthly intervals, with supplemental samples collected
156 during periods of high discharge. Approximately 200 measurements of DOC and POC were
157 obtained at each of the gauging sites over the 10-year span (Table 1), along with continuous
158 measurements of river discharge. For the James, the USGS data were supplemented by
159 measuring DIC and Cl at the Fall Line at 1-2 week intervals during 2012-2019 (189 samples
160 collected). Seasonal, inter-annual and discharge-dependent variation in riverine C concentrations
161 was analyzed using Generalized Additive Models (see Statistics). The models were used to

162 predict daily concentrations at each site, and, in combination with daily discharge, to derive daily
 163 loading values at the Fall Line. Local (ungauged) runoff was estimated as a constant fraction of
 164 the daily Fall Line discharge based on the proportion of catchment area represented by tributaries
 165 entering below the Fall Line. Daily concentrations were used in combination with Fall Line
 166 discharge, below Fall Line discharge, and total discharge to derive daily input and export fluxes.
 167 Daily fluxes were summed over the budget interval (typically 1-2 weeks) and used, in
 168 conjunction with the change in mass of Cl in the estuary between the start and end of each
 169 interval, to solve for the net tidal flux of Cl.

$$170 \quad \text{Estuary Cl Mass}_{t+1} = \text{Estuary Cl Mass}_t + \text{Riverine Cl} - \text{Export Cl} \pm \text{Net Tidal Cl} \quad (1)$$

171 The mass of Cl required to balance each budget interval was used in combination with
 172 measurements of Cl concentrations in tidal inflow and outflow, as represented by stations located
 173 on either side of the seaward boundary of our study reach (JMS69 and JMS56), to derive the
 174 effective volume of tidal exchange. This represents the volume of “new” water entering the
 175 study reach from the lower estuary with each tidal cycle. The James has an elongate shape that
 176 is typical of estuaries that occupy flooded river valleys. The back and forth of tidal flows means
 177 that the bulk of the water leaving on an outgoing tide returns on the subsequent incoming tide,
 178 and only a small proportion of the large tidal flux is “new” water. For the James, the effective
 179 volume of exchange is equivalent to 8% of the tidal prism (Bukaveckas and Isenberg 2013). For
 180 this study, estimates of the volume of tidal exchange were derived for each budget interval (N =
 181 309 for 2011-19). The effective volume of exchange was used along with measured C
 182 concentrations of tidal inflows and outflows to determine the net exchange of C at the seaward
 183 boundary of the study reach. Net tidal fluxes for each budget interval were aggregated to
 184 monthly values and presented as daily areal values for comparison to riverine input and export
 185 fluxes. Lastly, monthly estimates of estuarine C retention were derived based on the difference
 186 between input and output fluxes taking into account changes in mass storage within the estuary.

$$187 \quad \text{Estuary C Mass}_{t+1} = \text{Estuary C Mass}_t + \text{Riverine C} - \text{Export C} \pm \text{Net Tidal C} \pm \text{Retention} \quad (2)$$

188 For DIC, our estimation of retention also took into account air-water CO₂ exchange (see below).

189 2.5 Estuarine Metabolism. Previously published estimates of Gross Primary Production (GPP)
 190 and Ecosystem Respiration (ER) were used to assess internal C transformations for the James

191 and Pamunkey (Bukaveckas et al. 2020). Rates of metabolism were derived from continuous (15
192 min) monitoring of dissolved oxygen at stations located within our study segments of the James
193 and Pamunkey (Figure 1). The James monitoring station is located at the VCU Rice Center
194 Research Pier, approximately 2 km from our JMS75 sampling location. The Pamunkey station
195 (White House Landing) is operated by the Virginia Institute of Marine Science and located near
196 the mid-point of our study segment. Similar equipment (YSI 6600 or EXO sondes) and
197 protocols are used at the two stations including routine (2-3 week) maintenance and calibration
198 of sondes as per manufacturer recommendations. Daily GPP and ER were derived using the
199 single-station open-water method. Following Caffrey (2003; 2004), 15-minute DO
200 measurements were smoothed to 30-minute averages and multiplied by water depth to obtain
201 areal rates of oxygen flux at 30 minute intervals throughout the day.

$$202 \quad \text{O}_2 \text{ flux (g O}_2 \text{ m}^{-2} \text{ d}^{-1}) = (\text{DO}_{t2} - \text{DO}_{t1}) * \text{Water Depth} - \text{AE} \quad (3)$$

203 Atmospheric exchange (AE) was derived at 30-minute intervals based on water column DO
204 saturation and a generic estuarine gas transfer coefficient. A previous analysis using 23 years of
205 station data for the James showed that estimates of atmospheric exchange derived from oxygen
206 saturation and the fixed gas transfer coefficient were not significantly different from exchange
207 coefficients derived using variable water velocity and wind speed (Tassone and Bukaveckas
208 2019). ER was derived by extrapolating nightly O₂ fluxes to a 24-hour period. GPP was derived
209 as the sum of daytime oxygen production and ER during daylight hours. Oxygen-based values
210 were converted to C assuming a photosynthetic quotient of 1.2 and a respiratory quotient of 1.

211 2.6 Sampling and Analysis. Methods were described previously (Bukaveckas et al. 2011;
212 Bukaveckas et al. 2020; Henderson and Bukaveckas 2021) and are summarized here. Data were
213 collected from 4 stations in the James tidal fresh segment, 3 stations in each of the Pamunkey
214 and Mattaponi study reaches, and one tributary stream (Kimages Creek) located at the VCU Rice
215 Center (Figure 1; Table 1). Estuarine sites were sampled by boat in the main channel except in
216 the upper, narrow sections of the Pamunkey and Mattaponi where samples were collected from
217 shore in areas of active flow. Owing to vertically well-mixed conditions (no temperature or
218 salinity stratification) water samples and in situ measurements were obtained near the surface
219 (~0.5 m). Water temperature and salinity were measured using a YSI Pro DDS sonde. The
220 partial pressure of carbon dioxide in water and air was measured in the field using a PP Systems

221 EGM 4 portable infrared CO₂ analyzer calibrated at 0 and 2000 ppm. Water samples were
222 analyzed for chlorophyll-a (CHLa), POC, DIC, DOC and Cl. Samples for CHLa and POC were
223 filtered through Whatman GF/A glass filters (0.5-µm nominal pore size). Filters for CHLa
224 analyses were extracted for 18 h in buffered acetone and analyzed on a Turner Design TD-700
225 Fluorometer (Arar and Collins 1997). Filters for POC analysis were dried at 60 C for 48 h,
226 fumed with HCl to remove inorganic carbon and analyzed on a Perkin–Elmer CHN analyzer.
227 Chloride concentrations were determined using a Skalar segmented flow analyzer by the
228 ferricyanide method (APHA 1998). Samples for DIC and DOC were filtered in the field
229 through Whatman GF/A filters and analyzed using a Shimadzu TOC analyzer.

230 2.7 Air-Water CO₂ Fluxes. Air-water exchange of CO₂ was calculated using the equation from
231 Cai and Wang (1998):

$$232 \text{ Flux CO}_2 = K_T K_H (p\text{CO}_{2\text{-water}} - p\text{CO}_{2\text{-air}}) \quad (4)$$

233 where K_T is the gas transfer velocity, K_H is the solubility constant and $p\text{CO}_2$ is the partial
234 pressure of CO₂ in water and air. The solubility constant was derived according to the equation
235 of Weiss (1974) taking into account water temperature and salinity recorded at the time of CO₂
236 measurement. Gas transfer velocities were initially derived from daily average wind speed (U_{10}
237 corrected) measured at the VCU Rice Center Research Pier (James) and the Taskinas Creek
238 NERR station (Pamunkey and Mattaponi). Gas transfer velocities derived from wind speed
239 generally fell within the range of 1 to 1.5 m d⁻¹, which is low in comparison to the global average
240 (5.7 m d⁻¹, Raymond et al. 2017) and to values that are considered appropriate for large rivers
241 (4.3 m d⁻¹, Alin et al. 2011; Reiman and Xu 2019). Based on these considerations, a value of 4.3
242 m d⁻¹ was used for all calculations (see Discussion for further consideration of gas transfer
243 velocities).

244 2.8 Statistics. Generalized Additive Models (GAMs) were used to model river and estuarine C
245 and Cl concentrations based on discharge, day of year (to capture seasonal patterns) and decimal
246 date (to depict inter-annual variation). GAMs are gaining increasing usage for modeling water
247 chemistry due to their ability to account for non-linear effects and to fit trends of a form that is
248 not known *a priori* (Morton & Henderson 2008; Murphy et al. 2019; Yang and Moyer 2020;
249 Wiik et al. 2021). The GAM analysis was performed using the "mgcv" package in R (Wood
250 2006). The package default thin plate regression spline was used to depict the effect sizes of

251 discharge and decimal date; a cyclic cubic regression spline was used to depict seasonal effects.
252 The default output for the effect size was shifted to center on the mean of the modeled dependent
253 variable to show the response of the GAM model within the range of dependent variable values.

254

255 **3. Results**

256 3.1 Estuarine Hydrology

257 The James, Pamunkey and Mattaponi Rivers exhibit similar hydrographs with highest monthly
258 average discharge during January-May and lowest discharge in July-November (Figure 2).
259 Average monthly discharge in winter-spring is approximately 4-fold higher in comparison to
260 summer-fall. Median freshwater replacement times (FRT), taking into account Fall Line inputs
261 plus local (ungauged) tributaries, were 30 d (James), 46 d (Mattaponi) and 60 d (Pamunkey)
262 during the period of study. The mass of Cl in the James tidal fresh segment varied by >20-fold
263 from seasonal minimum values during high discharge ($\sim 7 \text{ mg L}^{-1}$) to peak values ($>100 \text{ mg L}^{-1}$)
264 during summer base flow (Figure 3). Despite the large seasonal variation, Cl changed relatively
265 slowly within the estuary (median = $0.5 \% \text{ d}^{-1}$). The gradual change in estuarine Cl belies the
266 underlying dynamics in which input and output fluxes largely offset. Riverine inputs (Fall Line
267 plus local) ranged from 1 to $3 \text{ g Cl m}^{-2} \text{ d}^{-1}$ over the seasonal cycle. These displaced a larger mass
268 of Cl (export = $2\text{-}5 \text{ g Cl m}^{-2} \text{ d}^{-1}$) owing to higher Cl concentrations in the estuary relative to river
269 inputs. In late summer (August-October), the development of strong Cl gradients across the
270 seaward boundary of the study reach resulted in high rates of Cl gain and loss via tidal exchange
271 (up to $10\text{-}20 \text{ g Cl m}^{-2} \text{ d}^{-1}$). As the lower tidal fresh segment accounts for the bulk of total volume
272 (80%), increases in Cl at the seaward end of the study reach had a large effect on estuarine Cl
273 mass. These seasonal increases in estuarine Cl were most pronounced in summers with low
274 freshwater inputs (e.g., 2012, 2017, 2019). By volume, the effective tidal exchange derived from
275 the Cl mass balance was equivalent to 7.4% (median) and $14 \pm 1\%$ (mean and SE) of the tidal
276 prism.

277 3.2 Discharge Effects on River and Estuarine C

278 Discharge was a significant factor influencing riverine C concentrations, though the strength of
279 these effects differed among C fractions and among the three tributaries. Increasing discharge

280 was associated with increasing river DOC in the Mattaponi (from 6 to 12 mg L⁻¹) and Pamunkey
281 (from 5 to 9 mg L⁻¹), but had little effect on James River DOC, which was generally low over the
282 range of observed discharge (3-4 mg L⁻¹; Figure 4). Generalized Additive Models incorporating
283 discharge, seasonal and inter-annual variation accounted for 50 to 81% of the variation in river
284 DOC (Table 2). Seasonal patterns were characterized by peak river DOC in summer and
285 minimum values in spring, with a seasonal range of 2-3 mg L⁻¹ (Supplemental Figure 1).
286 Increasing discharge was associated with large increases of POC in the James River (from 1 to
287 20 mg L⁻¹; Figure 4). Discharge accounted for the bulk of the variation in James River POC
288 (71%) with little additional variation explained by season or inter-annual effects (76% for full
289 model). The effects of discharge on river POC were weaker in the Mattaponi and Pamunkey,
290 where concentrations were generally low over the range of discharge (<2 and <4 mg L⁻¹,
291 respectively). Models incorporating discharge, seasonal and inter-annual variation accounted for
292 38% and 51% (respectively) of the variation in river POC at these sites (Supplemental Figure 2).
293 Increasing discharge was associated with large decreases in DIC of the James River (from 20 to
294 1 mg L⁻¹; Figure 4). The GAM analysis accounted for 44% of the variation in DIC at this site
295 (no river DIC data for Pamunkey and Mattaponi). Overall, increasing discharge resulted in
296 higher DOC concentrations in the Pamunkey and Mattaponi Rivers, higher POC concentrations
297 in the James River, and lower DIC concentrations in the James River.

298 Although increases in discharge had a positive effect on riverine DOC and POC, estuarine
299 concentrations were only weakly, and in some cases negatively affected by increasing discharge
300 (Figure 5). In the James, estuarine DOC concentrations were typically higher than riverine
301 values (Supplemental Figure 3), such that increases in river discharge resulted in a reduction in
302 estuarine DOC (from 7 to 2 mg L⁻¹). In the Pamunkey and Mattaponi, increasing discharge had
303 little effect on estuarine DOC as estuarine concentrations were similar to river concentrations
304 (Figure 5). Discharge was not a significant predictor of variation in DOC for the Pamunkey and
305 Mattaponi Estuaries (Table 2). Seasonal and inter-annual effects were also weak, resulting in a
306 low proportion of variation in estuarine DOC explained by the GAMs (13-27%). Similar
307 findings for POC showed weak seasonal, inter-annual and discharge dependent effects and a low
308 proportion of explained variation for the Pamunkey and Mattaponi Estuaries (40% and 14%,
309 respectively). In contrast, POC concentrations in the James Estuary were strongly influenced by
310 season, with predicted concentrations rising from 1 to 2 mg L⁻¹ during winter to summer. POC

311 concentrations were negatively related to discharge, declining by $\sim 0.5 \text{ mg L}^{-1}$ over the lower
312 range of discharge (up to $400 \text{ m}^3 \text{ s}^{-1}$). The overall model accounted for 75% of the variation in
313 POC for the James Estuary. Increasing discharge had a significant negative effect on DIC in all
314 three estuaries, which decreased by $5\text{-}6 \text{ mg L}^{-1}$ over the observed range of discharge. Seasonal
315 and inter-annual effects on estuarine DIC were weaker; the full models accounted for 68-76% of
316 the variation in estuarine DIC. Overall, these findings show that river discharge had strong
317 negative effects on estuarine DIC, but little influence on estuarine DOC and POC. Significant
318 seasonal variation in POC was observed in the James, but not the Pamunkey or Mattaponi.

319 3.3 Estuarine pCO₂

320 GAM analysis revealed significant seasonal and discharge-dependent variation in estuarine pCO₂
321 (Table 2). The effects of discharge on estuarine pCO₂ differed among the 3 tributaries (Figure
322 6). In the Pamunkey and Mattaponi, there was little effect of discharge, except in the upper
323 quartile of the range, which was associated with rising estuarine pCO₂. In the James, estuarine
324 pCO₂ increased linearly over the lower one-third range of discharge, and thereafter plateaued.
325 The Mattaponi and Pamunkey exhibited large seasonal variations in estuarine pCO₂. Peak
326 summer concentrations ($\sim 2600 \text{ ppmv}$) were two-fold higher in comparison to winter minimum
327 values ($\sim 1200 \text{ ppmv}$). A more complex seasonal pattern was observed in the James with bi-
328 model peaks in spring and fall (850 and 1250 ppmv , respectively) bracketing low concentrations
329 in mid-summer. In summer, significantly lower pCO₂ was observed at sites located at the CHLa
330 maximum (JMS75 = 789 ppmv , JMS69 = 644 ppmv) relative to stations in the upper tidal fresh
331 segment (JMS99 = 1007 ppmv) and the most seaward station (JMS56 = 909 ppmv ; $p < 0.01$).
332 The two stations located at the CHLa maximum were the only sites to exhibit periodic under-
333 saturation of pCO₂ (Supplemental Figure 4). The low values at these stations were not observed
334 in winter. There was little longitudinal variation in pCO₂ among stations in the Pamunkey and
335 Mattaponi. Overall, annual average concentrations in the Pamunkey ($2010 \pm 117 \text{ ppmv}$) and
336 Mattaponi ($1900 \pm 120 \text{ ppmv}$) were more than 2-fold higher relative to the James (784 ± 77
337 ppmv). Higher pCO₂ concentrations in the Pamunkey and Mattaponi estuaries were associated
338 with larger air-water CO₂ fluxes (2.97 ± 0.17 and $2.77 \pm 0.17 \text{ g C m}^{-2} \text{ d}^{-1}$, respectively) relative
339 to the James ($0.87 \pm 0.05 \text{ g C m}^{-2} \text{ d}^{-1}$; Figure 7). Strong seasonal patterns were observed in the

340 Pamunkey and Mattaponi with monthly average fluxes ranging from 1-2 g m⁻² d⁻¹ in winter to 3-
341 4 g m⁻² d⁻¹ in summer, whereas fluxes from the James were similar year-round (~1 g m⁻² d⁻¹).

342 3.4 C Fluxes & Retention

343 C fluxes into and out of the James Estuary varied seasonally (Figure 8). DOC inputs followed
344 expected seasonal patterns with peak values (1-2 g m⁻² d⁻¹) during months with elevated
345 discharge (January-May) and minimum values (~0.3 g m⁻² d⁻¹) during predominantly low
346 discharge in July-November. Seasonal variation in DOC inputs was closely matched by export
347 fluxes. Net tidal fluxes were negligible by comparison (-0.03 ± 0.01 g m⁻² d⁻¹) owing to small
348 differences in concentration across the segment boundary. Monthly DOC retention ranged from
349 -0.30 to 0.12 g m⁻² d⁻¹, and was generally negative, indicating net export of DOC. On an annual
350 basis, the DOC balance was -0.10 ± 0.02 g m⁻² d⁻¹, with export exceeding inputs by 11 ± 5%.
351 Riverine inputs of POC varied seasonally with highest values in January-May (0.5 to 1.9 g m⁻² d⁻¹)
352 and generally low values in June-December (< 0.3 g m⁻² d⁻¹). By contrast, estuarine export of
353 POC was consistently low throughout the year (< 0.5 g m⁻² d⁻¹). As a result, POC retention was
354 highest in January-May (0.3 to 1.5 g m⁻² d⁻¹). Net tidal fluxes were positive indicating a loss of
355 POC with each tidal cycle, but these fluxes were small (0.09 ± 0.03 g m⁻² d⁻¹) in comparison to
356 river inputs. On an annual basis, the net retention of POC was 0.59 ± 0.11 g m⁻² d⁻¹,
357 corresponding to 72 ± 4% of inputs. DIC input and output fluxes followed a similar pattern as
358 for DOC, with peak values in months with high discharge. Taking into account estuarine export
359 and atmospheric fluxes, the James was a net source of DIC with losses (4.25 g m⁻² d⁻¹) exceeding
360 inputs (2.82 g m⁻² d⁻¹) by 51%.

361 Our mass balance analysis does not explicitly consider the role of point source inputs in the
362 estuarine C budget. Point sources that discharge to the tidal fresh segment of the James are
363 principally wastewater treatment plants, and some industries associated with the Richmond
364 metro area. The volume of effluent discharged to the James is small (annual average = 15-21 m³
365 s⁻¹ during 2007-14) in comparison to annual average river discharge (~225 m³ s⁻¹). But as
366 effluent may contain elevated C concentrations, point sources could potentially contribute an
367 appreciable fraction of C inputs. Point sources typically do not report C concentrations as part of
368 their effluent monitoring, therefore we carried out a 2-year study of DIC, DOC and POC
369 concentrations in effluent from the largest point source (City of Richmond WWTP). Effluent

370 POC concentrations ($1.54 \pm 0.13 \text{ mg L}^{-1}$) were comparable to riverine values, whereas effluent
371 DOC ($13.1 \pm 1.2 \text{ mg L}^{-1}$) and DIC ($22.7 \pm 1.6 \text{ mg L}^{-1}$) were two-fold higher relative to riverine
372 concentrations. These values were extrapolated to all point source inputs to the James as a first
373 approximation of their potential importance to the estuarine C budget. Daily average POC loads
374 from point sources ($0.02 \text{ g m}^{-2} \text{ d}^{-1}$) were too small to appreciably affect our estimate of estuarine
375 POC retention. Point source inputs of DOC ($0.21 \text{ g m}^{-2} \text{ d}^{-1}$) and DIC ($0.36 \text{ g m}^{-2} \text{ d}^{-1}$) were
376 equivalent to 23% and 12% (respectively) of riverine inputs. Taking into account point source
377 contributions, the mass balance shows that the James tidal fresh segment is a net sink for DOC
378 ($0.12 \text{ g m}^{-2} \text{ d}^{-1}$) and POC ($0.61 \text{ g m}^{-2} \text{ d}^{-1}$) and a net source of DIC ($1.07 \text{ g m}^{-2} \text{ d}^{-1}$). Overall, the
379 James tidal fresh segment was nearly in balance (within 6%) for total C inputs and outputs.

380 Annual average DOC loads to the Pamunkey ($0.67 \pm 0.11 \text{ g m}^{-2} \text{ d}^{-1}$) and Mattaponi (0.89 ± 0.12
381 $\text{g m}^{-2} \text{ d}^{-1}$) were similar to the James ($0.91 \pm 0.12 \text{ g m}^{-2} \text{ d}^{-1}$) on an areal basis. Seasonal variation
382 in DOC inputs followed patterns in discharge with peak values ($0.7 - 1.7 \text{ g m}^{-2} \text{ d}^{-1}$) in winter-
383 spring and minimum values ($0.2 - 0.7 \text{ g m}^{-2} \text{ d}^{-1}$) in summer-fall (Figure 9). Export fluxes closely
384 matched river inputs on a seasonal basis, and balanced to within 10% on an annual basis.
385 Riverine POC inputs to the Pamunkey and Mattaponi (0.17 ± 0.03 and $0.14 \pm 0.02 \text{ g m}^{-2} \text{ d}^{-1}$,
386 respectively) were considerably lower relative to the James ($0.81 \pm 0.15 \text{ g m}^{-2} \text{ d}^{-1}$). For the
387 James, POC inputs were nearly equal to DOC inputs, whereas for the Pamunkey and Mattaponi,
388 DOC accounted for the bulk of OC inputs (79% and 86%, respectively). Export of POC from
389 the Pamunkey and Mattaponi matched inputs to within 10% on an annual basis.

390 3.5 Estuarine Metabolism

391 Rates of GPP and ER were compared to standing stocks (areal values) of DIC and POC to assess
392 the potential influence of C fixation and remineralization on estuarine C concentrations (Figure
393 10). In the James, GPP and ER followed expected seasonal patterns with peak values ($3.5 - 4.0$
394 $\text{g C m}^{-2} \text{ d}^{-1}$) during June-September and low values ($<1 \text{ g C m}^{-2} \text{ d}^{-1}$) in colder months. GPP and
395 ER tracked closely throughout the year, with ER exceeding GPP in colder months, and being
396 equal, or occasionally smaller (June-July) than GPP in warmer months. C fluxes associated with
397 GPP and ER were small in comparison to ambient concentrations of DIC, which ranged from 30
398 to 40 g m^{-2} . By contrast, POC production via GPP was comparable to ambient concentrations of
399 POC, which ranged from 3 g m^{-2} in colder months to 6 g m^{-2} in warmer months. Metabolism of

400 the Pamunkey Estuary was lower and more heterotrophic in comparison to the James. ER varied
401 seasonally from 0.5 to 1.8 g C m⁻² d⁻¹, whereas GPP was persistently low throughout the year (<
402 0.5 g C m⁻² d⁻¹). Standing stocks of DIC were large by comparison, ranging from 10 to 40 g m⁻².
403 GPP was small in comparison to standing stocks of POC (3 to 5 g m⁻²).

404 **4.0 Discussion**

405 4.1 Riverine C Inputs & Estuarine Concentrations

406 An analysis of C dynamics in the upper portions of the James, Mattaponi and Pamunkey
407 estuaries revealed differences in dominant forms of C and variable responses to changes in river
408 discharge. The James was dominated by products of mineral weathering as DIC accounted for
409 73% of total C with smaller contributions from DOC (20%) and POC (7%). By contrast, organic
410 forms accounted for a larger fraction (49%) of total C in the Pamunkey and Mattaponi. These
411 differences are attributed to variable contributions from local (Coastal Plain) vs. upland
412 (Mountain and Piedmont) runoff. The James Estuary receives inputs from a large catchment
413 with the bulk of runoff (90%) derived from above the Fall Line. By contrast, the Pamunkey and
414 Mattaponi Estuaries receive a greater proportion of their inputs from local tributaries situated
415 within the Coastal Plain. Local floodplains and tidal marshes contribute DOC, while the
416 predominantly sandy soils of the Coastal Plain have low capacity for retaining DOC, and
417 contribute little DIC. Differences in source waters may also account for contrasting response in
418 river and estuarine C to high discharge events. Larger increases in POC were observed during
419 discharge events in the James, relative to the Pamunkey and Mattaponi. Prior studies
420 documented higher sediment yields from Mountain and Piedmont regions in comparison to the
421 Coastal Plain (Gellis et al. 2009). In the James River, changes in C concentrations with
422 increasing discharge were asynchronous as DIC was negatively related to discharge, whereas
423 POC showed a positive relationship. These findings suggest that DIC export from the watershed
424 is limited by weathering rates (source limited) whereas POC export is transport limited (Wymore
425 et al. 2021). For DIC, this resulted in a dilution response in both the river and estuary, whereas
426 high discharge resulted in a flushing response (enrichment) of POC in the river and estuary.
427 Dilution of estuarine DIC during high discharge was also reported in the nearby Delaware
428 Estuary and linked to reductions in acid neutralizing capacity and greater sensitivity to
429 acidification (Joesef et al. 2017). For DOC, a strong flushing response was observed in the

430 Pamunkey and Mattaponi Rivers, but not the James. Higher DOC concentrations following
431 storm events has been attributed to greater leaching from soils due to higher water elevation and
432 soil inundation (Zarnetske et al. 2018; Patrick et al. 2020). The extensive wetlands and
433 floodplains along the Mattaponi and Pamunkey likely serve as source areas for DOC. Prior work
434 showed that differences in source waters played a role in determining underwater light
435 conditions in these estuaries, as light attenuation in the James was strongly regulated by
436 suspended particulate matter, whereas dissolved organic matter had a greater role in attenuating
437 light in the Pamunkey and Mattaponi estuaries (Henderson and Bukaveckas 2021). Overall, our
438 findings showed strong concentration-discharge relationships in riverine waters, whereas
439 estuarine responses were weaker and more variable. Inter-estuarine differences in C forms and
440 response to discharge were linked to differences in the physiographic setting of the estuarine
441 catchments.

442 4.2 C Mass Balance

443 The tidal freshwater segment of the James Estuary was a net sink for POC and DOC, and a net
444 source of DIC. On an annual basis, external organic matter inputs were attenuated by 28% (± 3)
445 within the tidal fresh segment. The mass balance indicates that a high proportion (72%) of POC
446 inputs were retained in the tidal fresh segment and that retention of POC accounted for the bulk
447 (84%) of organic matter retention. Amann et al. (2012) similarly documented high retention of
448 POC in tidal freshwaters of the River Elbe. The transition from fluvial to tidal conditions favors
449 the settling of suspended particulate matter, which contained ~10-20% organic matter
450 (Bukaveckas et al. 2019). Peak retention occurred during periods of elevated discharge when
451 inputs of particulate matter to the estuary were highest. Our findings do not support the view
452 that inland waters function primarily as transport systems (“pipes”) during periods of elevated
453 discharge (Zarnetske et al. 2018) as the bulk of organic matter retention occurred during high
454 flows in winter, and was associated with the retention of particulates. High retention of
455 particulate C is consistent with prior results showing that peak retention of N and P occurred
456 during colder months with elevated river discharge (Bukaveckas and Isenberg 2013). Retention
457 of dissolved N and P was highest during low discharge in summer, but this accounted for a
458 relatively small proportion of total N and P retention on an annual basis. For C, as for N and P,
459 the mass of particulate matter delivered to the estuary during high discharge appears to be the

460 most important determinant of the amount retained within the estuary. The counter-intuitive
461 finding that peak retention occurs during periods of high transport (when “pipe” conditions
462 might prevail) is based on a consideration of the fate of both dissolved and particulate organic
463 matter, as the former largely passes through, while the latter is highly retained. The retention of
464 particulate matter reflects the underlying hydrodynamics of estuaries, and lakes, where the rapid
465 dissipation of fluvial forces promotes high retention of particulate matter during periods of
466 elevated discharge.

467 For the James, atmospheric losses were a small component of the C budget, equivalent to 18% of
468 riverine total C inputs and 15% of total C export. Volta et al. (2016) similarly report that CO₂
469 loss via evasion was ~15% of C export from North Sea estuaries. By contrast, CO₂ evasion from
470 the Pamunkey and Mattaponi was appreciably greater (by 3-fold) relative to the James. Our
471 pCO₂ concentrations for the Pamunkey were similar to those previously reported by Raymond et
472 al. (2000), whereas our air-water flux values were higher (~3 g C m⁻² d⁻¹ vs. ~0.7 g C m⁻² d⁻¹).
473 Comparisons of CO₂ fluxes are complicated by uncertainty regarding atmospheric exchange
474 (Raymond and Cole 2001; Borges et al. 2004; Raymond et al. 2017; Ward et al. 2017).
475 Raymond et al. (2000) used what they considered a conservative exchange coefficient (1.1 m d⁻¹
476 ¹). More recent studies have adopted higher exchange coefficients, particularly for systems
477 where tidal and fluvial forces likely play a greater role in determining boundary layer conditions
478 than are predicted from wind-based models. Wind speeds are low in the upper segments of these
479 estuaries because the prevailing winds (SSW) are nearly perpendicular to the long axis of the
480 channel, which runs mostly east-west. Turbulence generated by strong tidal forces in shallow
481 channels likely plays a greater role in influencing boundary conditions for gas exchange
482 (Raymond and Cole 2001; Borges et al. 2004). These conditions support the use of higher
483 exchange coefficients than would be derived from wind speed alone.

484 Tidal fluxes were not a large component of the mass balance for any of the C fractions.
485 Although the volume of water exchanged during a tidal cycle was large (tidal prism = 28% of
486 estuarine volume), the elongate shape of the estuary dictates that water leaving on an out-going
487 tide returns on the subsequent in-coming tide. Results from the Cl mass balance suggest that the
488 net tidal exchange was ~7% of the tidal prism, equivalent to 2% of estuarine volume. In

489 addition, weak C gradients across the lower boundary of the study reach indicate that tidal inputs
490 and outputs largely offset.

491 4.3 Metabolism & Carbon

492 Mass balance and metabolism data provide independent evidence that these estuaries are net
493 heterotrophic. The mass balance indicates that the James is a sink for organic C and a source of
494 inorganic C, consistent with metabolism data showing that ecosystem respiration exceeds GPP.
495 Greater heterotrophy was observed in the Pamunkey where respiration rates were comparable to
496 the James, but GPP was substantially lower. This finding was consistent with the observed
497 higher CO₂ concentrations and efflux. The evasion of CO₂ from the Pamunkey and Mattaponi
498 was large (3x) in comparison to riverine inputs of DOC and POC, whereas CO₂ loss from the
499 James was ~50% of riverine OM inputs. Greater heterotrophy of the former is attributed to
500 differences in hydrogeomorphology and forms of primary production. Higher chlorophyll-a
501 values in the James indicate greater phytoplankton contributions to GPP, which brings the tidal
502 fresh segment more closely in balance with respect to production and respiration. The
503 Pamunkey and Mattaponi have low chlorophyll-a by comparison (Bukaveckas et al. 2020) but
504 extensive lateral floodplains and emergent marshes (Hupp et al. 2009; Noe and Hupp 2009; Lake
505 et al. 2013). Decomposition of terrestrial organic matter during floodplain inundation may
506 account for the high CO₂ concentrations and air-water fluxes during high discharge conditions.
507 Van Dam et al. (2018) similarly reported that high CO₂ losses during flooding events accounted
508 for 30-40% of annual emissions from North Carolina estuaries. An accounting of changes in
509 floodplain C stores before and after inundation events is needed to better understand their role in
510 supporting respiration in these systems. Organic matter inputs following senescence of emergent
511 vegetation may also contribute to higher rates of respiration and CO₂ evasion. Emergent plant
512 production would not be captured in the diel dissolved-O₂ based estimates of ecosystem GPP,
513 which may over-estimate heterotrophy in this system. Overall, C mass balance and ecosystem
514 metabolism data show that the upper segments of these estuaries are net heterotrophic. This
515 finding is consistent with a meta-analysis of metabolism data showing that estuaries are
516 generally net heterotrophic (Hoellein et al. 2013), but contrasts with recent work by Brodeur et
517 al. (2019) showing that the Susquehanna River and mainstem Chesapeake Bay are a net sink for
518 DIC, and therefore net autotrophic. In the case of Chesapeake Bay, it may be that much of the

519 terrestrial organic matter (or at least, the POC fraction) is captured in the tributaries, thereby
520 favoring a prevalence of autochthony over allochthony, and GPP in excess of R.

521 Despite the large riverine influence in these upper estuarine segments, internal cycling of C via
522 production and respiration was large in comparison to external forcing via fluvial and tidal
523 exchange (Figure 11). In summer, remineralization of C via respiration was almost 2-fold
524 greater in comparison to external DIC inputs. In winter, the balance tipped strongly in favor of
525 external inputs as riverine DIC contributions were 3-fold greater than internal production via
526 respiration. Internal production of POC via GPP was an order of magnitude higher than external
527 inputs of POC in summer. In winter, GPP contributions were approximately equal to external
528 inputs of POC. Based on GPP, the estimated turnover time of the POC pool was 1.5 d in
529 summer. Taking into account that 60% of POC in the James is algal (Wood et al. 2016), the
530 estimated phytoplankton turnover time was 0.9 d. The high rates of internal biological
531 processing relative to through-puts of C places the James toward the lake-end, rather than the
532 stream-river end, on the metabolism and residence time spectrum (Hotchkiss et al. 2018). This is
533 likely a consequence of tidal conditions, which allow for longer water residence time compared
534 to non-tidal rivers. Proximal nutrient inputs (from riverine and point sources) and poor water
535 clarity (due to suspended sediments), likely also contribute to the dominance of phytoplankton
536 over aquatic plants in this system. If recent increases in water clarity continue (Henderson and
537 Bukaveckas 2021), we would expect a shift toward macrophyte dominance, lower GPP:ER, and
538 a diminished influence of internal C cycling.

539 The tidal fresh segment of the James has moderately low DIC and high GPP, which raises the
540 question whether primary production is limited by the availability of inorganic C. Our data show
541 that daily autotrophic C demand is small (~10%) relative to the available DIC pool. In summer,
542 DIC requirements to sustain GPP exceed the rate of external supply via river inputs, but
543 remineralization of C via respiration is approximately equal to GPP, indicating that internal
544 cycling is sufficiently large to preclude C limitation. However, a case could be made for
545 potential C limitation of photosynthesis due to depletion of pCO₂. The diffusion of CO₂ in water
546 occurs more slowly than in air, potentially resulting in depletion during periods of high
547 autotrophic demand. In the James, low CO₂, with occasional under-saturation, was observed in
548 summer at stations corresponding to the CHLa maximum. Other studies in riverine settings have

549 shown that phytoplankton can reduce CO₂ to near or below atmospheric equilibrium (Raymond
550 et al. 1997; Crawford et al. 2017). As CO₂ is energetically favored for carbon fixation, depletion
551 of CO₂ may reduce production efficiency and alter community structure by favoring taxa capable
552 of using bicarbonates. A number of prior studies have linked primary production and pCO₂
553 (Jansson et al. 2012; Low-Decarie et al. 2015; Hasler et al. 2016). Our CO₂ data were collected
554 mid-morning, closer to the diel maximum than the afternoon minimum (Crosswell et al. 2017;
555 Reiman and Xu 2019), thereby potentially under-estimating CO₂ depletion. The possibility that
556 phytoplankton-driven CO₂ depletion in the James may affect production and community
557 composition cannot be discounted, though this effect appears limited to mid-summer and stations
558 located at the CHLa maximum.

559 4.4 C Sources & Consumer Energetics

560 Lastly, I consider the utility of our C mass balance for understanding trophic energetics of the
561 James food web, particularly with respect to autochthony and allochthony. Combining mass
562 balance, ecosystem metabolism and bioenergetics is a potentially powerful approach to
563 advancing our understanding of C cycles, but there are few examples, often, as in this case, due
564 to a lack of data on consumer production (Ruegg et al. 2021). From a mass flux perspective, a
565 comparison of autochthonous ($GPP = 719 \pm 32 \text{ g C m}^{-2} \text{ y}^{-1}$) and allochthonous ($POC = 298 \pm 56$,
566 $DOC = 340 \pm 44 \text{ g C m}^{-2} \text{ y}^{-1}$) inputs suggests that internal C sources are nearly equal ($54 \pm 4\%$)
567 to external inputs, despite the large riverine influence in the upper estuary. These estimates can
568 be refined to better reflect availability for consumers by discounting GPP by 40% to reflect loss
569 via autotrophic respiration (Ruegg et al. 2021) and taking into account the fraction of POC and
570 DOC that is retained ($28 \pm 3\%$). By this estimate, autochthonous production contributes 70%
571 ($431 \text{ g C m}^{-2} \text{ y}^{-1}$) and allochthonous inputs 30% ($203 \text{ g C m}^{-2} \text{ y}^{-1}$) of C available to consumers.
572 These percentages are based on annualized values though their relative importance varies
573 seasonally with the majority of GPP occurring in May to October, and the bulk of POC delivered
574 in January to May.

575 Comparisons of mass fluxes may not be indicative of C supporting secondary production if
576 consumers preferentially utilize one source over another. A number of studies have suggested
577 that autochthonous sources account for a disproportionately large fraction of C assimilation due
578 to the higher nutritional quality of algae over partially decomposed terrestrial plant matter (Brett

579 et al. 2009; Thorp and Bowes 2017). Stable isotope analysis of the James food web has shown
580 that the dominant metazoans by biomass, which are benthic omnivores (catfish, adult gizzard
581 shad), carry a predominantly terrestrial C signature, whereas zooplankton and planktivorous fish
582 (juvenile gizzard shad and threadfin shad) were dependent on autochthonous C sources (Wood et
583 al. 2016). These patterns were consistent with analysis of basal resources showing that the
584 sediments in the estuary were largely (90%) comprised of terrestrial C, whereas seston contained
585 a greater fraction of autochthonous C (60% in summer).

586 The lack of secondary production data does not allow us to align C supply from autochthonous
587 and allochthonous sources with C demands of consumers. However, the rate of biomass removal
588 for one of the dominant metazoans (catfish) can be used as a first approximation of their annual
589 production. Catfish were introduced to the James during the 1970's and 1980's and now
590 dominate the fishery (Fabrizio et al. 2018), which has led to questions about their influence on
591 food webs and ecosystem processes (Greenlee and Lim 2011; Hilling et al. 2019; Schmitt et al.
592 2019). The biomass of catfish removed from the James represents a conservative estimate of
593 their annual production in that current harvest rates have not brought about declines in the catfish
594 population, indicating that annual production exceeds the amount of biomass removed (Orth et
595 al. 2017). During 2010-2020, the commercial harvest of catfish in the tidal James averaged
596 1,000,000 lbs y^{-1} (data provided by Virginia Marine Resources Commission), which taking into
597 account the area of the fresh-brackish estuary, yields a harvest rate of 8.6 kg $ha^{-1} y^{-1}$. In addition
598 to the commercial harvest, piscivorous birds are an important component of biomass removal.
599 Here we focus on predation by bald eagles and osprey as there are census data during the
600 breeding season (from areal surveys) and estimates of catfish contributions to adult and nestling
601 diets (from direct observations and stable isotopes; Garman et al. 2010). Based on census data
602 and bioenergetics modeling, fish consumption by bald eagles and osprey was estimated at 0.6 kg
603 $ha^{-1} d^{-1}$ for the James tidal fresh segment. Taking into account the contribution of catfish to the
604 diet of bald eagles and osprey (~35%) yields an estimate of catfish biomass removal of 77 kg ha^{-1}
605 y^{-1} , which is ~9-fold higher than for commercial fisheries. With further corrections for the
606 moisture content (75%; Cresson et al. 2017) and C content of fish tissues (45%; Tanner et al.
607 2000), the total catfish removal by birds and commercial fishing is 0.96 g C $m^{-2} y^{-1}$. Their
608 trophic position in the James (trophic level = 3.1; Orth et al. 2017) suggests a production
609 efficiency of ~1% (Ruegg et al. 2021), which yields an estimated C demand to maintain this

610 level of production/harvest of $96 \text{ g C m}^{-2} \text{ y}^{-1}$. The C demand for this introduced species
611 corresponds to 15% of C available to consumers from allochthonous and autochthonous sources.
612 Stable isotope data indicate that catfish in the James tidal fresh obtain 9% of their C from
613 autochthonous sources and 81% from allochthonous sources (Wood et al. 2016). Applying these
614 values suggests that 2% of GPP and 41% of allochthonous inputs are required to sustain current
615 levels of catfish biomass removal from the James tidal fresh. The high rate of utilization for
616 allochthonous inputs is consistent with our prior finding that consumer-mediated recycling is an
617 important component of nutrient supply, and may account for the lack of response in primary
618 production to large reductions in point source nutrient inputs (Wood et al. 2014).

619 4.5 Summary

620 Relatively complete C budgets are relatively rare, in part due to the effort involved in quantifying
621 C fluxes from various sources (Hanson et al. 2015). This paper provides an accounting of C
622 fluxes at the river-estuarine transition for three tributaries of Chesapeake over a span of years
623 and discharge conditions. The findings show that the relative importance of external (river
624 inputs & tidal exchange) vs. internal (metabolism) drivers differed among the three estuaries
625 based on their physiographic setting and forms of primary production. Estuarine C forms were
626 influenced by variable contributions from upland (DIC-rich, POC-rich) and lowland (DOC-rich)
627 sources. Peak organic matter retention was associated with trapping of POC during high
628 discharge conditions. Tidal exchange was not an important component of the C budget, whereas
629 biological transformations via production and respiration were large in the phytoplankton-
630 dominated James Estuary. Contrary to expectations, autochthonous sources accounted for the
631 bulk of organic matter inputs despite the large riverine influence on the upper estuary.
632 Commercial harvest data and previously derived estimates of piscivory by birds provided a basis
633 for estimating consumer C demand, albeit for a single dominant species, and at a coarse
634 (annualized) scale. Further progress in aligning C flows to food web energetics depends on the
635 availability of production data for a greater range of consumers and at shorter time intervals.
636 Bringing together C mass balance, ecosystem metabolism and consumer production data would
637 enable a potentially powerful approach for advancing our understanding of how the timing and
638 sources of C inputs constrain trophic energetics.

639

640 Acknowledgements

641 Thanks to Samantha Rogers who drafted figures for this paper, to D. Hopler, S. Tassone and W.
642 M. Lee who carried out the field and lab work, and to Donald Orth for helpful discussions
643 regarding catfish in the James. I am grateful to the USGS for providing discharge, DOC and
644 POC data for Fall Line stations and to the Virginia Institute of Marine Science for making
645 available dissolved oxygen data from the Pamunkey. This paper is dedicated to Jon Cole for his
646 contributions to our understanding of C cycling in inland waters and in appreciation for his
647 ability to turn numbers into interesting stories.

648 Data availability

649 Data can be accessed upon request to the corresponding author.

650 Competing interests

651 The author declares that there is no conflict of interest.

652

653 Reference List

- 654
655 Alin, S. R., de Fatima, F.L., Rasera, M., Salimon, C.I., Richey, J.E., Holtgrieve, G.W., Krusche,
656 A.V. and Snidvongs, A. Physical controls on carbon dioxide transfer velocity and flux in
657 low-gradient river systems and implications for regional carbon budgets. *Journal of*
658 *Geophysical Research: Biogeosciences* 116: G01009, 2011
- 659 Amann, T., Weiss, A. and Hartmann, J. Carbon dynamics in the freshwater part of the Elebe
660 estuary, Germany: Implications of improving water quality. *Estuarine, Coastal and Shelf*
661 *Science* 107: 112-121, 2012.
- 662 Amann, T., Weiss, A. and Hartmann, J. Inorganic carbon fluxes in the inner Elbe Estuary,
663 Germany. *Estuaries and Coasts* 38: 192-210, 2015.
- 664 Basu, B. K., and Pick, F.R. Factors regulating phytoplankton and zooplankton biomass in
665 temperate rivers. *Limnology and Oceanography* 41: 1572-1577, 1996.
- 666 Bianchi, T. S. The role of terrestrially derived organic carbon in the coastal ocean: a changing
667 paradigm and the priming effect. *Proceedings of the National Academy of Sciences USA*
668 108: 19473-19481, 2011.
- 669 Borges, A. V., Delille, B., Schiettecatte, L-S., Gazeau, F., Abril, G. and Frankignoulle, M. Gas
670 transfer velocities of CO₂ in three European estuaries (Randers Fjord, Scheldt, and
671 Thames). *Limnology and Oceanography* 49: 1630-1641, 2004.
- 672 Brett, M. T., Kainz, M., Taipale, S. and Seshan, H. Phytoplankton, not allochthonous carbon,
673 sustains herbivorous zooplankton production. *Proceedings of the National Academy of*
674 *Sciences USA* 106: 21197-21201, 2009.
- 675 Brodeur, J. R., Chen, B., Su, J., Xu, Y-Y., Hussain, N., Scaboo, K.M., Zhang, Y., Testa, J.M. and
676 Cai, W-J. Chesapeake Bay inorganic carbon: distribution and seasonal variability.
677 *Frontiers in Marine Science* 6: 99, 2019.
- 678 Bukaveckas, P. A., Barry, L.E., Beckwith, M.J., David, V. and Lederer, B. Factors determining
679 the location of the chlorophyll maximum and the fate of algal production within the tidal
680 freshwater James River. *Estuaries and Coasts* 34: 569-582, 2011.
- 681 Bukaveckas, P. A., and Isenberg, W.N. Loading, transformation and retention of nitrogen and
682 phosphorus in the tidal freshwater James River (Virginia). *Estuaries and Coasts* 36: 1219-
683 1236, 2013.
- 684 Bukaveckas, P. A., and Wood, J.D. Nitrogen retention in a restored tidal stream (Kimages
685 Creek, VA) assessed by mass balance and tracer approaches. *Journal of Environmental*
686 *Quality* 43: 1614-1623, 2014.
- 687 Bukaveckas, P. A., Beck, M., Devore, D. and Lee, W.M. Climate variability and its role in
688 regulating C, N and P retention in the James River Estuary. *Estuarine, Coastal and Shelf*
689 *Science* 205: 161-173, 2018.
- 690 Bukaveckas, P. A., Katarzyte, M., Schlegel, A., Spuriene, R., Egerton, T.A. and Vaiciute, D.
691 Composition and settling properties of suspended particulate matter in estuaries of the
692 Chesapeake Bay and Baltic Sea regions. *Journal of Soils and Sediments* 19: 2580-2593,
693 2019.

- 694 Bukaveckas, P. A., Tassone, S., Lee, W.M. and Franklin, R.B. The influence of storm events on
695 metabolism and water quality of riverine and estuarine segments of the James, Mattaponi
696 and Pamunkey Rivers. *Estuaries and Coasts* 43: 1585-1602, 2020.
- 697 Butman, D., Stackpoole, S., Stets, E.G., McDonald, C.P., Clow, D.W. and Striegl, R.G. Aquatic
698 carbon cycling in the conterminous United States and implications for terrestrial carbon
699 accounting. *Proceedings of the National Academy of Sciences USA* 113: 58-63, 2016.
- 700 Caffrey, J. M. Production, respiration and net ecosystem metabolism in U.S. estuaries.
701 *Environmental Monitoring and Assessment* 81: 207-219, 2003.
- 702 Caffrey, J. M. Factors controlling net ecosystem metabolism in U.S. estuaries. *Estuaries* 27: 90-
703 101, 2004.
- 704 Cai, W.-J., and Wang, Y. The chemistry, fluxes and sources of carbon dioxide in the estuarine
705 waters of the Satilla and Altamaha Rivers, Georgia. *Limnology and Oceanography* 43:
706 657-668, 1998.
- 707 Cole, J. J., Prairie, Y.T., Caraco, N.F., McDowell, W.H., Tranvik, L.J., Striegl, R.G., Duarte,
708 C.M., Kortelainen, P., Downing, J.A., Middelburg, J.J. and Melack, J.M. Plumbing the
709 global carbon cycle: integrating inland waters into the terrestrial carbon budget.
710 *Ecosystems* 10: 171-184, 2007.
- 711 Crawford, J. T., Butman, D., Loken, L.C., Stadler, P., Kuhn, C. and Striegl, R.G. Spatial
712 variability of CO₂ concentrations and biogeochemistry in the Lower Columbia River.
713 *Inland Waters* 7: 417-427, 2017.
- 714 Cresson, P., Travers-Trolet, M., Rouquette, M., Timmerman, C-A., Giraldo, C., Lefebvre, S. and
715 Ernande, B. Underestimation of chemical contamination in marine fish muscle tissue can
716 be reduced by considering variable wet:dry weight ratios. *Marine Pollution Bulletin*.
717 123: 279-285, 2017.
- 718 Crosswell, J. R., Anderson, I.C., Stanhope, J.W., Van Dam, B., Brush, M.J., Ensign, S.H.,
719 Piehler, M.F., McKee, B., Bost, M. and Paerl, H.W. Carbon budget of a shallow
720 lagoonal estuary: transformations and source-sink dynamics along the river-estuary-ocean
721 continuum. *Limnology and Oceanography* 62: S29-S45, 2017.
- 722 Fabrizio, M. C., Tuckey, T.D., Latour, R.J., White, G.C. and Norris A.J. Tidal habitats support
723 large numbers of invasive blue catfish in a Chesapeake Bay sub-estuary. *Estuaries and*
724 *Coasts* 41: 827-840, 2018.
- 725 Garman, G., Viverette, C., Watts, B. and Macko. S. Predator-prey Interactions among Fish-
726 eating Birds and selected Fishery Resources in the Chesapeake Bay: Temporal and
727 Spatial Trends and Implications for Fishery Assessment and Management. William &
728 Mary Center for Conservation Biology Technical Report #349.
729 https://scholarworks.wm.edu/ccb_reports/349, 2010.
- 730 Gellis, A.C. and others. Sources, transport, and storage of sediment in the Chesapeake Bay
731 Watershed. U.S. Geological Survey Scientific Investigations Report 2008-5186, 2009.
- 732 Greenlee, R. S., and Lim, C.N. Searching for equilibrium: population parameters and variable
733 recruitment in introduced blue catfish populations in four Virginia tidal river systems.
734 *American Fisheries Society Symposium* 77: 349-367, 2011.

- 735 Hanson, P. C., Pace, M.L., Carpenter, S.R., Cole, J.J. and Stanley, E.H. Integrating landscape
736 carbon cycling: research needs for resolving organic carbon budgets of lakes. *Ecosystems*
737 18: 363-375, 2015.
- 738 Hasler, C. T., Butman, D., Jeffrey, J.D. and Suski, C.D. Freshwater biota and rising pCO₂?
739 *Ecology Letters* 19: 98-108, 2016.
- 740 Henderson, R. and Bukaveckas, P.A. Factors governing light attenuation in upper segments of
741 the James and York Estuaries and their influence on primary producers. *Estuaries &*
742 *Coasts* <https://doi.org/10.1007/s12237-021-00983-6>, 2021.
- 743 Hilling, C. D., Bunch, A.J., Emmel, J.A., Schmitt, J.D. and Orth, D.J. Growth and mortality of
744 invasive flathead catfish in the tidal James River, Virginia. *Journal of Fish and Wildlife*
745 *Management* 10: 641-652, 2019.
- 746 Hoellein, T. J., Bruesewitz, D.A. and Richardson, D.C. Revisiting Odum (1956): a synthesis of
747 aquatic ecosystem metabolism. *Limnology and Oceanography* 58: 2089-2100, 2013.
- 748 Hoffman, J. C., Bronk, D.A. and Olney, J.E. Organic matter sources supporting lower food web
749 production in the tidal freshwater portion of the York River estuary. *Estuaries and Coasts*
750 31: 898-911, 2008.
- 751 Hotchkiss, E. R., Sadro, S. and Hanson, P.C. Toward a more integrative perspective on carbon
752 metabolism across lentic and lotic inland waters. *Limnology and Oceanography: Letters*
753 3: 57-63, 2018.
- 754 Hoitink, A. J. F. and Jay, D.A. Tidal river dynamics: implications for deltas. *Reviews of*
755 *Geophysics* 54: 240-272, 2016.
- 756 Holgerson, M. A. and Raymond, P.A. Large contribution to inland water CO₂ and CH₄
757 emissions from very small ponds. *Nature Geoscience* doi: 10.1038/ngeo2654, 2016.
- 758 Hupp, C. R., Pierce, A.R. and Noe, G.B. Floodplain geomorphic processes and environmental
759 impacts of human alteration along Coastal Plain rivers, USA. *Wetlands* 29: 413-429,
760 2009.
- 761 Jansson, M., Karlsson, J. and Jonsson, A. Carbon dioxide super-saturation promotes primary
762 production in lakes. *Ecology Letters* 15: 527-532, 2012.
- 763 Joesoef, A., Kirchman, D.L., Sommerfield, C.K. and Cai, W-J. Seasonal variability of the
764 inorganic carbon system in a large coastal plain estuary. *Biogeosciences* 14: 4949-4963,
765 2017.
- 766 Jones, A. E., Hodges, B.R., McClelland, J.W., Hardison, A.K. and Moffett, K.B. Residence-
767 time-based classification of surface water systems. *Water Resources Research* 53: 5567-
768 5584, 2017.
- 769 Jones, A. E., Hardison, A.K., Hodges, B.R., McClelland, J.W. and Moffett, K.B. Defining a
770 riverine tidal freshwater zone and its spatiotemporal dynamics. *Water Resources*
771 *Research* 56: e2019WRR026619, 2020.
- 772 Lake, S.J., Brush, M.J., Anderson, I.C. and Kator, H.I. Internal versus external drivers of
773 periodic hypoxia in a coastal plain tributary estuary: the York River, Virginia. *Marine*
774 *Ecology Progress Series* 492: 21-39, 2013.

- 775 Lionard, M., Muylaert, K., Hanoutti, A., Maris, T., Tackx, M. and Vyverman W. Inter-annual
776 variability in phytoplankton summer blooms in the freshwater tidal reaches of the
777 Schelde estuary (Belgium). *Estuarine, Coastal and Shelf Science* 79: 694-700, 2008.
- 778 Low-Decarie, E., Bell, G. and Fussman, G.F. CO₂ alters community composition and response
779 to nutrient enrichment of freshwater phytoplankton. *Oecologia* 177: 875-883, 2015.
- 780 Lucas, L. V., Thompson, J.K. and Brown, L.R. Why are diverse relationships observed between
781 phytoplankton biomass and transport time? *Limnology and Oceanography* 54: 381-390,
782 2009.
- 783 Meybeck, M. Global analyses of river systems: from Earth system controls to Anthropocene
784 syndromes. *Phil. Trans. R. Soc. Lond. B* 358: 1935-1955, 2003.
- 785 Middelburg, J. J., and Herman, P.M.J. Organic matter processing in tidal estuaries. *Marine*
786 *Chemistry* 106: 127-147, 2007.
- 787 Morton, R. and Henderson, B.L. Estimation of non-linear trends in water quality: an improved
788 approach using generalized additive models. *Water Resources Research* 44: W07420,
789 2008.
- 790 Murphy, R. R., Perry, E., Harcum, J. and Keisman, J. A Generalized Additive Model approach
791 to evaluating water quality: Chesapeake Bay case study. *Environmental Modelling and*
792 *Software* 118: 1-13, 2019.
- 793 Muylaert, K., Tackx, M. and Vyverman, W. Phytoplankton growth rates in the tidal freshwater
794 reaches of the Schelde estuary (Belgium) estimated using a simple light-limited primary
795 production model. *Hydrobiologia* 540: 127-140, 2005.
- 796 Noe, G. B. and Hupp, C.R. Retention of riverine sediment and nutrient loads by Coastal Plain
797 floodplains. *Ecosystems* 12: 728-746, 2009.
- 798 Orth, D.J., Jiao, Y., Schmidt, J.D., Hilling, C.D., Emmel J.A. and Fabrizio, M.C. Dynamics and
799 Role of Non-native Blue Catfish *Ictalurus furcatus* in Virginia's Tidal Waters. Final
800 Report submitted to Virginia Department of Game and Inland Fisheries. DOI:
801 10.13140/RG.2.2.35917.54246, 2017.
- 802 Pace, M. L., Findlay, S.E.G. and Lints, D. Zooplankton in advective environments: the Hudson
803 River community and a comparative analyses. *Canadian Journal of Fisheries and Aquatic*
804 *Sciences* 49: 1060-1069, 1992.
- 805 Patrick, C. J. and others. A system level analysis of coastal ecosystem responses to hurricane
806 impacts. *Estuaries and Coasts* 43: 943-959, 2020.
- 807 Qin, Q. and Shen, J. The contribution of local and transport processes to phytoplankton biomass
808 variability over different time scales in the Upper James River, Virginia. *Estuarine,*
809 *Coastal and Shelf Science* 196: 123-133, 2017.
- 810 Raymond, P. A., Bauer, J.E. and Cole, J.J. Atmospheric CO₂ evasion, dissolved inorganic
811 carbon production, and net heterotrophy in the York River estuary. *Limnology and*
812 *Oceanography* 45: 1707-1717, 2000.
- 813 Raymond, P. A., Caraco, N.F. and Cole, J.J. Carbon dioxide concentration and atmospheric flux
814 in the Hudson River. *Estuaries* 20: 381-390, 1997.

- 815 Raymond, P. A. and Cole, J.J. Gas exchange in rivers and estuaries: Choosing a gas transfer
816 velocity. *Estuaries* 24: 312-317, 2001.
- 817 Raymond, P. A., Hartmann, J., Lauerwald, R., Sobek, S., McDonald, C.P., Hoover, M., Butman,
818 D., Striegl, R.G., Mayorga, E., Humborg, C., Kortelainen, P., Durr, H., Meybeck, M.,
819 Ciais, P. and Guth, P. Global carbon dioxide emissions from inland waters. *Nature* 503:
820 355-359, 2017.
- 821 Reiman, J. H. and Xu, Y.J. Diel variability of PCO₂ and CO₂ outgassing from the lower
822 Mississippi River: implications for riverine CO₂ outgassing estimation. *Water* 11: 43,
823 2019.
- 824 Richey, J. E., Melack, J.M., Aufdenkampe, A., Ballester, V.M. and Hess, L.L. Outgassing from
825 Amazonian rivers and wetlands as a large tropical source of atmospheric CO₂. *Nature*
826 416: 617-620, 2002.
- 827 Robson, B. J., Bukaveckas, P.A. and Hamilton, D.P. Modelling and mass balance assessments
828 of nutrient retention in a seasonally-flowing estuary (Swan River Estuary, Western
829 Australia). *Estuarine, Coastal and Shelf Science* 76: 282-292, 2008.
- 830 Ruegg, J., Conn, C.C., Anderson, E.P., Battin, T.J., Bernhardt, E.S., Canadell, M.B., Bonjour,
831 S.M., Hosen, J.D., Marzolf, N.S. and Yackulic, C.B. Thinking like a consumer: linking
832 aquatic basal metabolism and consumer dynamics. *Limnology and Oceanography*:
833 *Letters* 6: 1-17, 2021.
- 834 Schmitt, J. D., Peoples, B.K., Castello, L. and Orth, D.J. Feeding ecology of generalist
835 consumers: a case study of invasive blue catfish *Ictalurus furcatus* in Chesapeake Bay,
836 Virginia, USA. *Environmental Biology of Fishes* 102: 443-465, 2019.
- 837 Sellers, T. and Bukaveckas, P.A. Phytoplankton production in a large, regulated river: A
838 modeling and mass balance assessment. *Limnology and Oceanography* 48: 1476-1487,
839 2003.
- 840 Shen, J. and Lin, J. Modeling study of the influences of tide and stratification on age of water in
841 the tidal James River. *Estuarine, Coastal and Shelf Science* 68: 101-112, 2006.
- 842 Soballe, D. M. and Kimmel, B.L. A large-scale comparison of factors influencing phytoplankton
843 abundance in rivers, lakes, and impoundments. *Ecology* 68: 1943-1954, 1987.
- 844 Steen, A.D., Quigley L.M. and Buchan, A. Evidence for the priming effect in a planktonic
845 estuarine microbial community. *Frontiers in Marine Science* 3:6.
846 doi:10.3389/fmars.2016.00006, 2015.
- 847 Tassone, S. and Bukaveckas, P.A. Seasonal, interannual and longitudinal patterns in estuarine
848 metabolism derived from diel oxygen data using multiple computational approaches.
849 *Estuaries and Coasts* 42: 1032-1051, 2019.
- 850 Thorp, J. H. and Bowes, R.E. Carbon sources in riverine food webs: new evidence from amino
851 acid isotope techniques. *Ecosystems* 20: 1029-1041, 2017.
- 852 Tranvik, L. J., Downing, J.A., Cotner, J.B. and others. Lakes and reservoirs as regulators of
853 carbon cycling and climate. *Limnology and Oceanography* 54: 2298-2314, 2009.

- 854 Tranvik, L. J., Cole, J.J. and Prairie, Y.T. The study of carbon in inland waters - from isolated
855 ecosystems to players in the global carbon cycle. *Limnology and Oceanography: Letters*
856 3: 41-48, 2018.
- 857 Van Dam, B. R., Crosswell, J.R. and Paerl, H.W. Flood-driven CO₂ emissions from adjacent
858 North Carolina estuaries during Hurricane Joaquin (2015). *Marine Chemistry* 207: 1-12,
859 2018.
- 860 Vincent, W. F., Dodson, J.J., Bertrand, N. and Frenette, J-J. Photosynthetic and bacterial
861 production gradients in a larval fish nursery: The St. Lawrence River transition zone.
862 *Marine Ecology Progress Series* 139: 227-238, 1996.
- 863 Volta, C., Laruelle, G.G. and Regnier, P. Regional carbon and CO₂ budgets of North Sea tidal
864 estuaries. *Estuarine, Coastal and Shelf Science* 176: 76-90, 2016.
- 865 Vorosmarty, C. J., Meybeck, M., Fekete, B.M., Sharma, K.P., Green, P. and Syvitski, J.P.M.
866 Anthropogenic sediment retention: major global impact from registered river
867 impoundments. *Global and Planetary Change* 39: 169-190, 2013.
- 868 Ward, N. D. and others. The reactivity of plant-derived organic matter and the potential
869 importance of priming effects in the lower Amazon River. *JGR-Biogeosciences* 121:
870 1522–1539, 2016.
- 871 Ward, N. D., Bianchi, T.S., Medeiros, P.M., Seidel, M., Richey, J.E., Keil, R.G. and Sawakuchi,
872 H.O. Where carbon goes when water flows: carbon cycling across the aquatic
873 continuum. *Frontiers in Marine Science* 4: 7, 2017.
- 874 Wiik, E., Haig, H.A., Hayes, N.M., Finlay, K., Simpson, G.L., Vogt, R.J. and Leavitt, P.R.
875 Generalized additive models of climatic and metabolic controls of subannual variation in
876 pCO₂ in productive hardwater lakes. *Journal of Geophysical Research: Biogeosciences*
877 123: 1940-1959, 2021.
- 878 Wood, J. D. and Bukaveckas, P.A. Increasing severity of phytoplankton nutrient limitation
879 following reductions in point source inputs to the tidal freshwater segment of the James
880 River Estuary. *Estuaries and Coasts* 37: 1188-1201, 2014.
- 881 Wood, J. D., Elliott, D., Garman, G.C., Hopler, D., Lee, W.M., McIninch, S., Porter, A.J. and
882 Bukaveckas, P.A. Autochthony, allochthony and the role of consumers in influencing the
883 sensitivity of aquatic systems to nutrient enrichment. *Food Webs* 7: 1-12, 2016.
- 884 Wood, S. *Generalized Additive Models: an Introduction with R*, 1 ed. Chapman and Hall/CRC,
885 Boca Raton, FL, 2006.
- 886 Wymore, A. S., Fazekas, H.M. and McDowell, W.H. Quantifying the frequency of synchronous
887 carbon and nitrogen export to the river network. *Biogeochemistry* 152: 1-12, 2021.
- 888 Xu, X. and others. Tidal freshwater zones as hotspots for biogeochemical cycling: sediment
889 organic matter decomposition in the lower reaches of two South Texas rivers. *Estuaries*
890 *and Coasts* 44 : 722-733, 2021.
- 891 Yang, G. and Moyer, D.L. Estimation of non-linear water quality trends in high-frequency
892 monitoring data. *Science of the Total Environment* 715: 136686, 2020.

-
- 893 Young, M., Hoew, E., O'Rear, T., Berridge, K. and Moyle, P. Food web fuel differs across
894 habitats and seasons of a tidal freshwater estuary. *Estuaries and Coasts* 44: 286-301,
895 2021.
- 896 Zarnetske, J. P., Bouda, M., Abbott, B.W., Saiers, J. and Raymond, P.A. Generality of
897 hydrologic transport limitation of watershed organic carbon flux across ecoregions of the
898 United States. *Geophysical Research Letters* 45: 11702-11711, 2018.

899 Table 1. Data collection sites for this study include USGS Fall Line gauging stations (Q denotes
 900 discharge), estuarine sampling sites and an ungauged Coastal Plain tributary of the James
 901 (Kimages Creek). Station numbers denote distance in river miles from the confluence with
 902 Chesapeake Bay (James) or the York (Pamunkey and Mattaponi). Observations denote the
 903 number of sampling dates for water chemistry within the specified time span.

Tributary	Segment	Stations	Parameters	Years	Observations	Source
James	River	JMS110	Q, DOC, POC	2010-19	197	USGS (02037500)
		JMS110	Cl, DIC, pCO ₂	2012-19	189	This Study
	Estuary	JMS99,75,69,56	Cl, DOC, POC, DIC, pCO ₂	2015-19	105	This Study
	Ungauged	Kimages Creek	Cl, DOC, POC, DIC, pCO ₂	2012-19	211	This Study
Pamunkey	River	PMK82	Q, DOC, POC	2010-19	202	USGS (01673000)
	Estuary	PMK50,39,6	DOC, POC, DIC, pCO ₂	2017-19	60	This Study
Mattaponi	River	MPN54	Q, DOC, POC	2010-19	203	USGS (01674500)
	Estuary	MPN36,29,4	DOC, POC, DIC, pCO ₂	2017-19	60	This Study

904

905

906 Table 2. GAM analysis of seasonal (day of year; DOY), inter-annual (date) and discharge
 907 dependent variation in river, tributary and estuarine DOC, POC, DIC, pCO₂ and Cl. Data are for
 908 riverine and upper estuarine segments of the James, Mattaponi and Pamunkey as well as a local
 909 (below Fall Line) tributary (Kimages Creek). Statistics include the adjusted R², root mean
 910 square error (RMSE as mg L⁻¹, except pCO₂ = ppmv), and significance of s values with their
 911 effective degrees of freedom (** denotes p < 0.001; * p < 0.05).

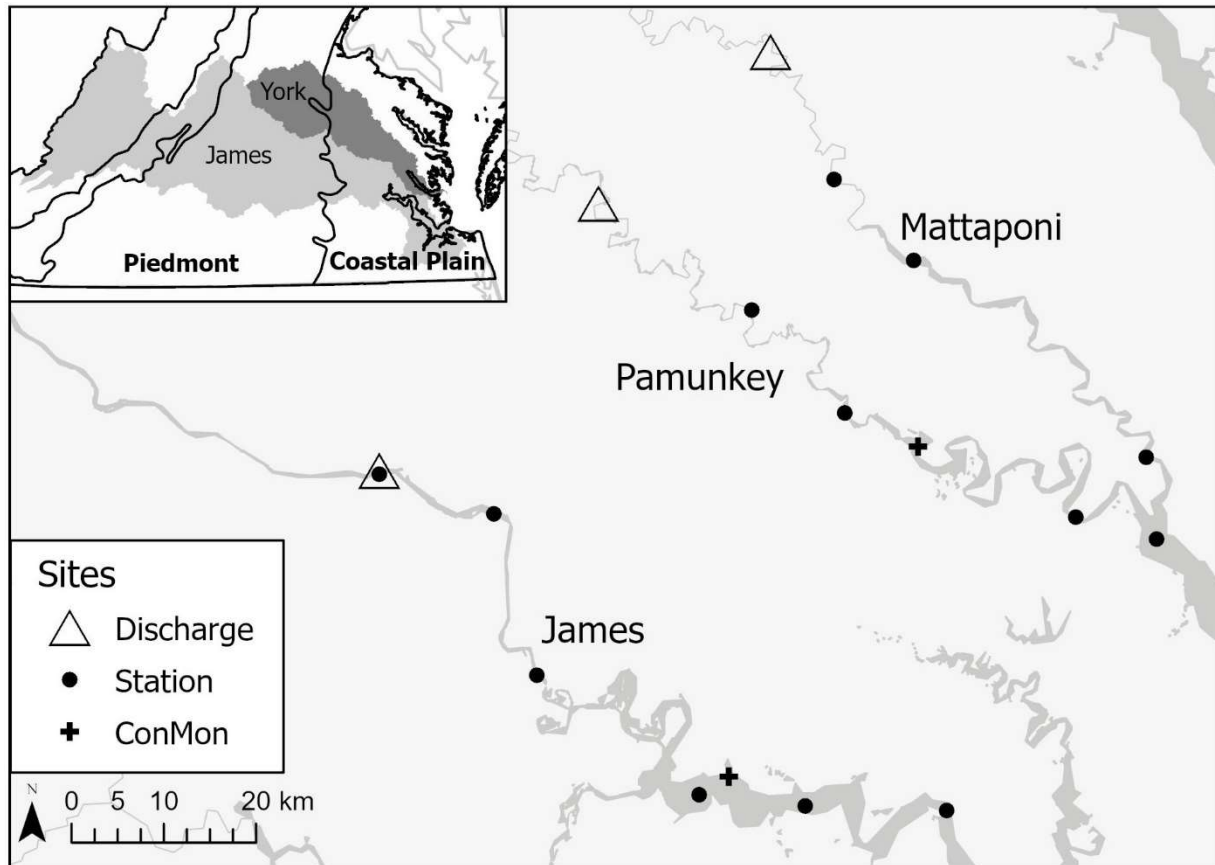
912

Model	Fraction	Site	Adj R ²	RMSE	s(DOY)	s(date)	s(discharge)
River	DOC	James	0.50	0.82	3.42**	8.52**	3.00**
		Mattaponi	0.81	1.00	5.66**	8.93**	5.43**
		Pamunkey	0.67	1.06	4.64**	8.61**	5.54**
	POC	James	0.76	1.74	3.67**	7.89**	8.20**
		Mattaponi	0.38	0.61	3.99**	6.34	6.25**
		Pamunkey	0.51	1.08	2.39**	8.95**	7.79**
	DIC	James	0.44	4.19	2.42**	7.89**	8.20**
pCO ₂	James	0.67	149	3.37**	6.43**	3.59**	
Cl	James	0.48	4.36	7.23**	8.30**	6.73**	
Tributary	DOC	Kimages	0.33	3.22	4.70**	8.26**	NA
	POC	Kimages	0.24	0.57	4.61**	7.63**	NA
	DIC	Kimages	0.19	3.00	0.41	8.26**	NA
	Cl	Kimages	0.23	8.63	6.46**	6.48**	NA
Estuary	DOC	James	0.13	3.44	4.29	1.96	1.91*
		Mattaponi	0.27	2.37	5.65	3.42**	1.00
		Pamunkey	0.27	2.61	5.94*	3.95**	1.00
	POC	James	0.75	0.22	5.77**	2.64**	3.68**
		Mattaponi	0.14	0.53	1.79*	1.00	4.13**
		Pamunkey	0.40	0.30	2.46**	1.27	7.59**
	DIC	James	0.76	1.55	1.27**	4.41**	2.50**
		Mattaponi	0.74	2.05	1.74**	2.27**	1.48**
		Pamunkey	0.68	2.10	1.30*	3.16**	1.00**
	pCO ₂	James	0.40	241	5.84**	3.48	2.38*
Mattaponi		0.82	367	3.31**	2.65**	4.14**	
Pamunkey		0.81	357	3.81**	2.73**	4.01**	
Cl	James	0.46	24.7	6.26**	8.54**	6.97**	

913

914

915 Figure 1. Map showing USGS discharge gauging locations, estuarine sampling sites and
916 continuous dissolved oxygen monitoring locations on the Mattaponi, Pamunkey and James.
917 Inset: James and York watersheds in relation to physiographic provinces.



918

Figure 2. Seasonal variation in instantaneous discharge measured at the Fall Line of the James, Mattaponi and Pamunkey Rivers. Here and in subsequent figures, symbols denote median (bar), 25 and 75 %-tiles (box), 5 and 95 %-tiles (whiskers) and outliers (dots).

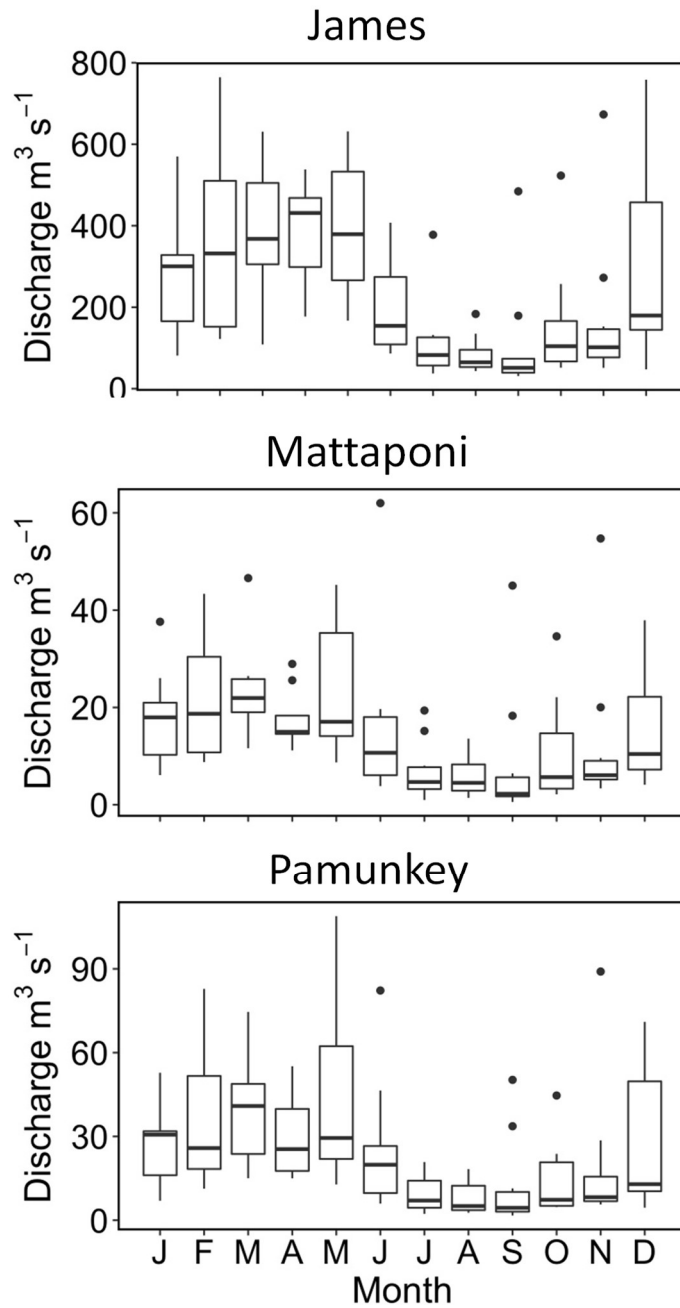


Figure 3. Time series of Cl concentrations in the tidal fresh segment of the James Estuary (upper panel) and Cl fluxes associated with river inputs, estuarine export and net tidal exchange (lower panels).

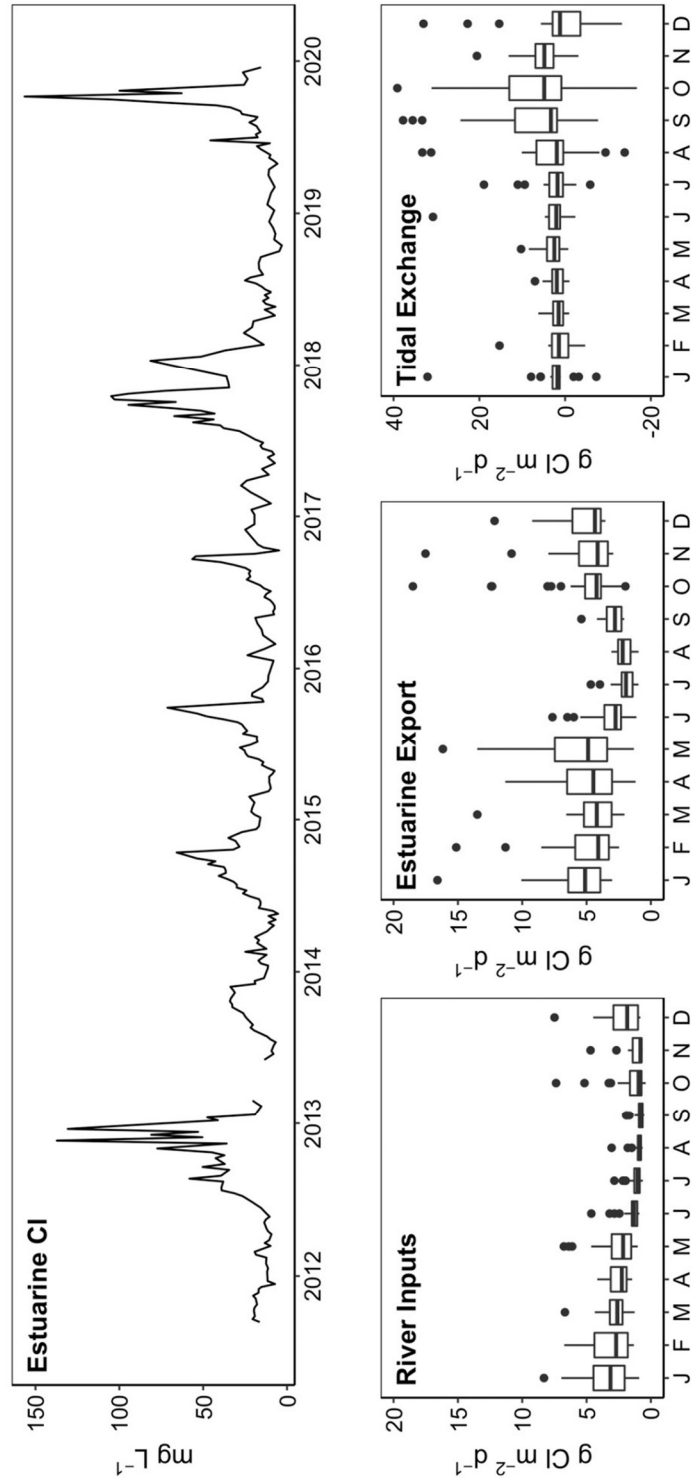


Figure 4. Results from GAM analysis depicting changes in riverine DOC, POC and DIC as a function of discharge (Q) for the James Mattaponi and Pamunkey Rivers.

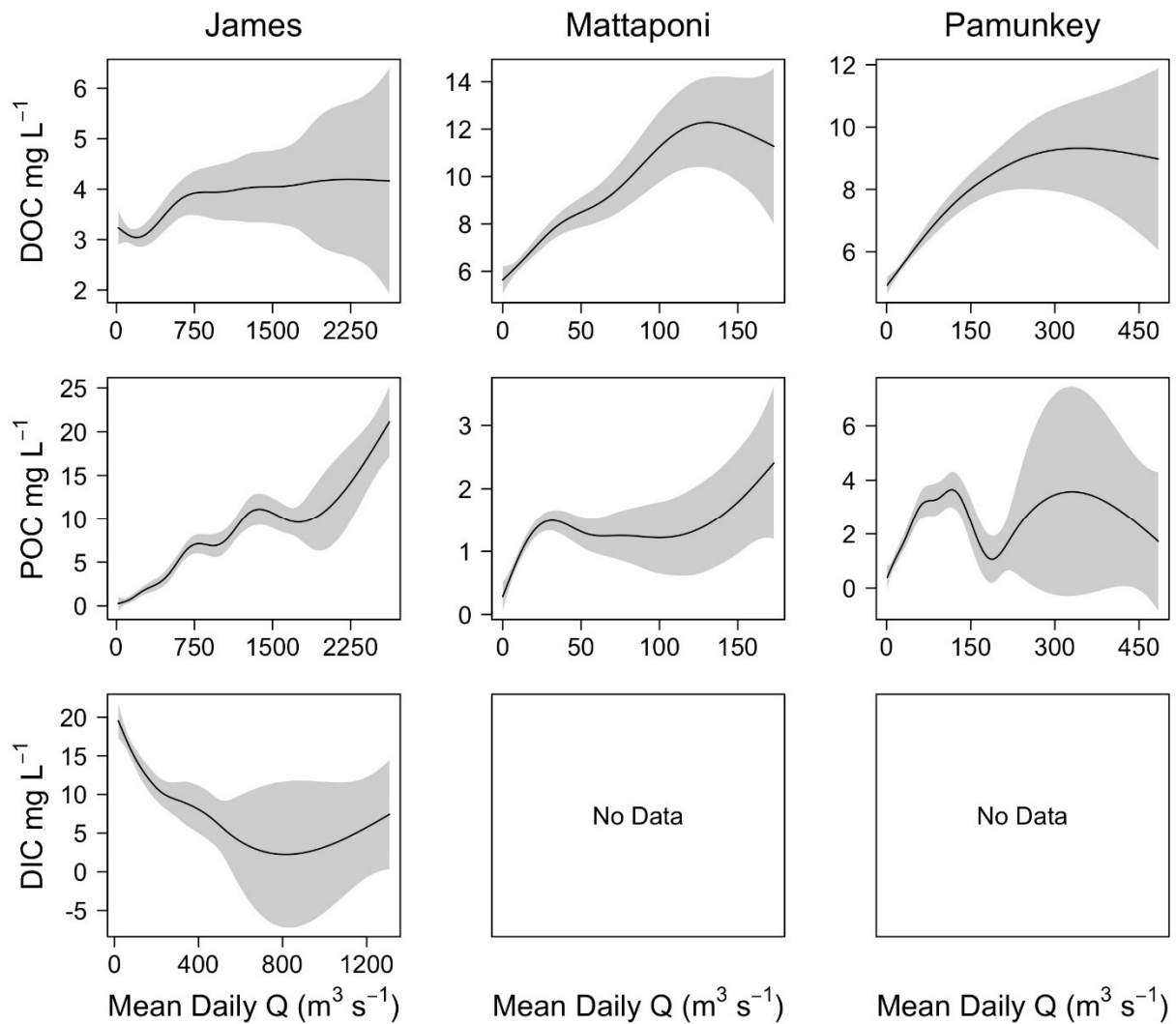


Figure 5. Results from GAM analysis depicting the effects of discharge (Q) on estuarine DOC, POC and DIC for the James Mattaponi and Pamunkey Estuaries. Concentrations are volume-weighted averages among estuarine sampling locations.

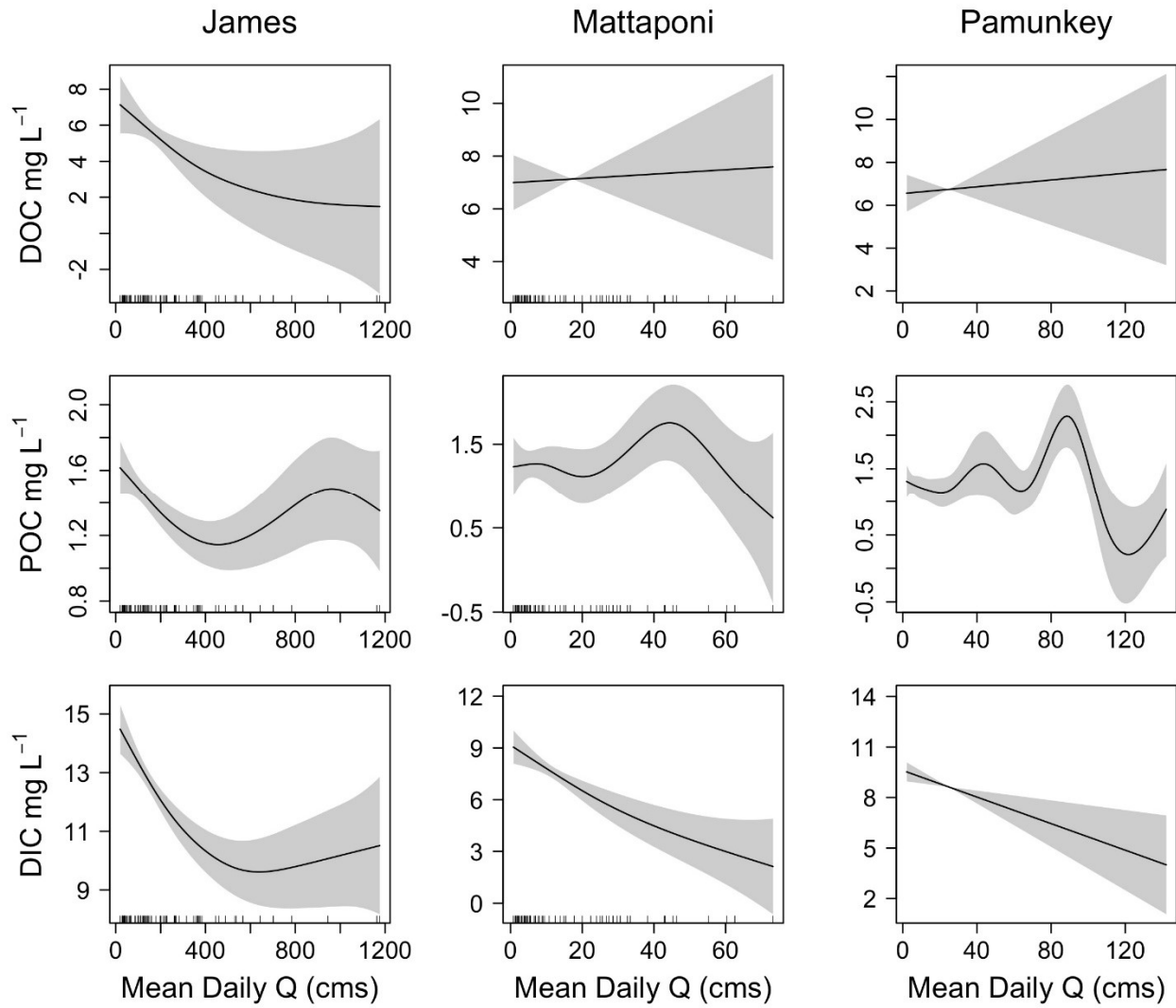


Figure 6. Results from GAM analysis depicting seasonal (day of year; DOY), inter-annual (decimal date) and discharge dependent variation in pCO₂ of the James, Mattaponi and Pamunkey Estuaries. Analyses were based on volume-weighted averages from 3-4 sampling locations in each estuary.

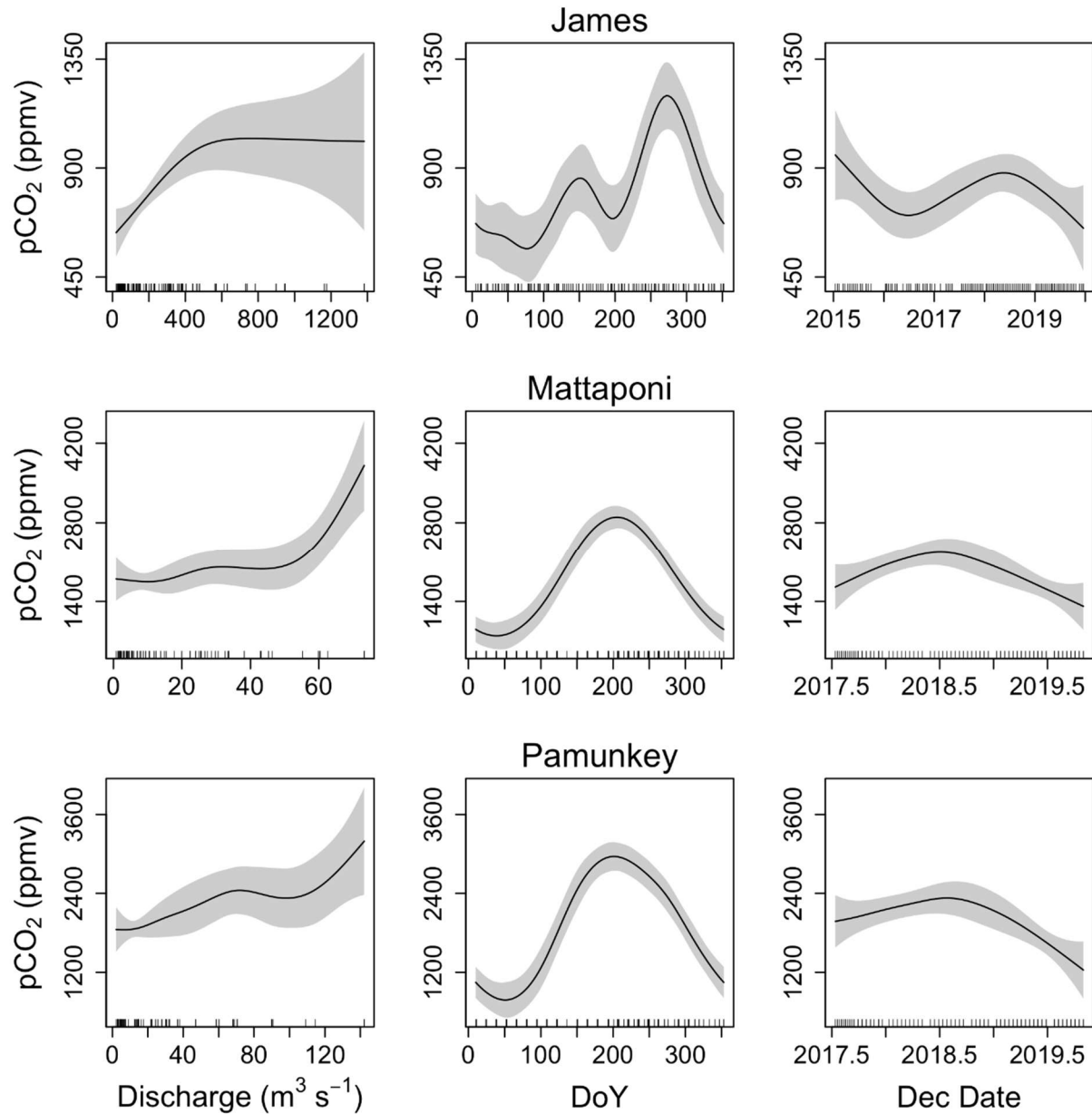


Figure 7. Monthly average values of air-water CO₂ fluxes for the James, Mattaponi and Pamunkey Estuaries. Positive values denote efflux of CO₂ from the estuary.

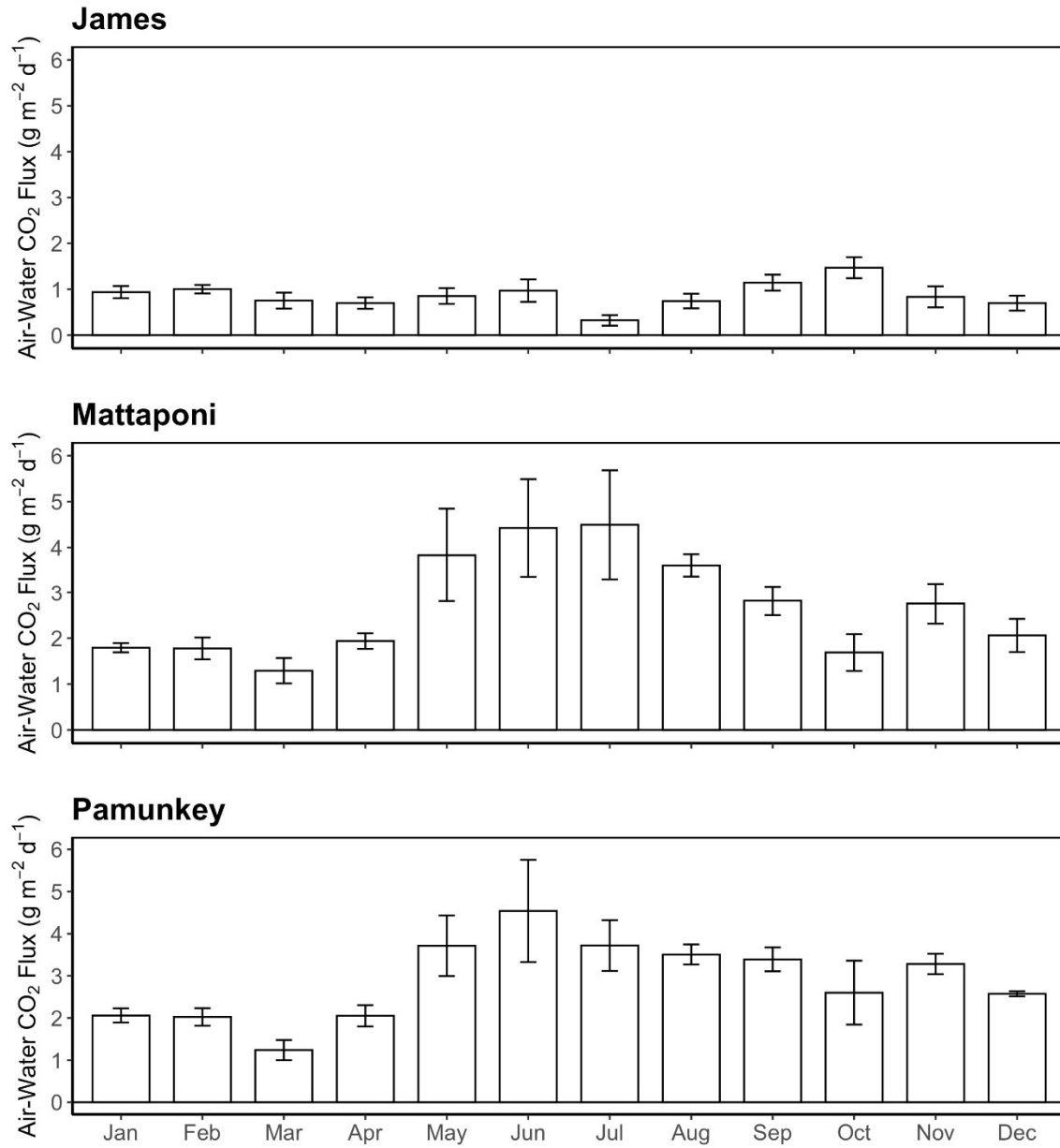


Figure 8. Seasonal variation in DOC, POC and DIC fluxes associated with riverine inputs, estuarine export, tidal exchange and estuarine retention for the tidal freshwater segment of the James Estuary (note differences in y axis scaling). Negative values for estuarine retention denote a net loss. DIC retention estimates take into account atmospheric losses of CO₂.

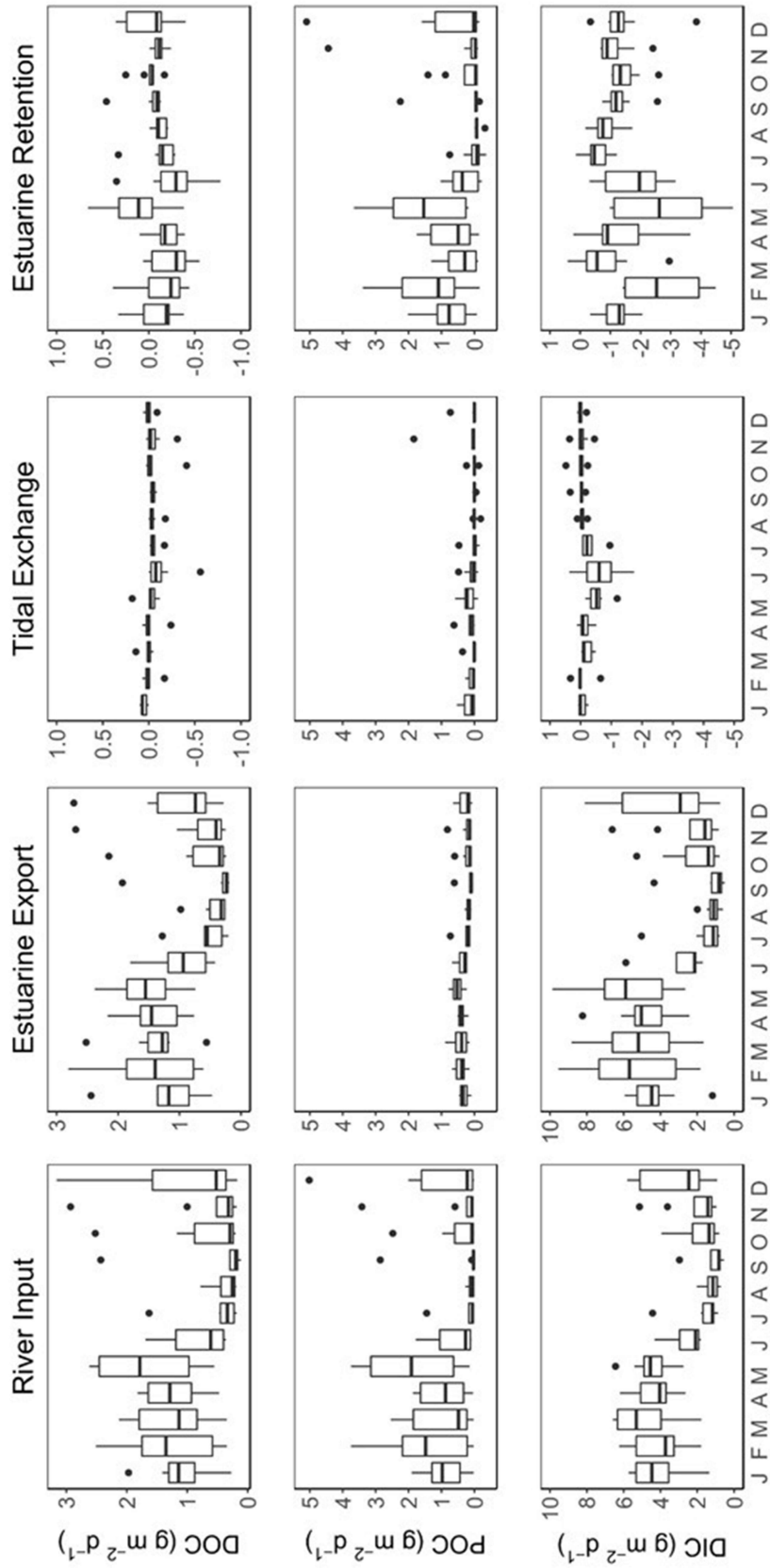


Figure 9. River input and estuarine export fluxes of DOC and POC for the Pamunkey (PMK) and Mattaponi (MPN) estuaries.

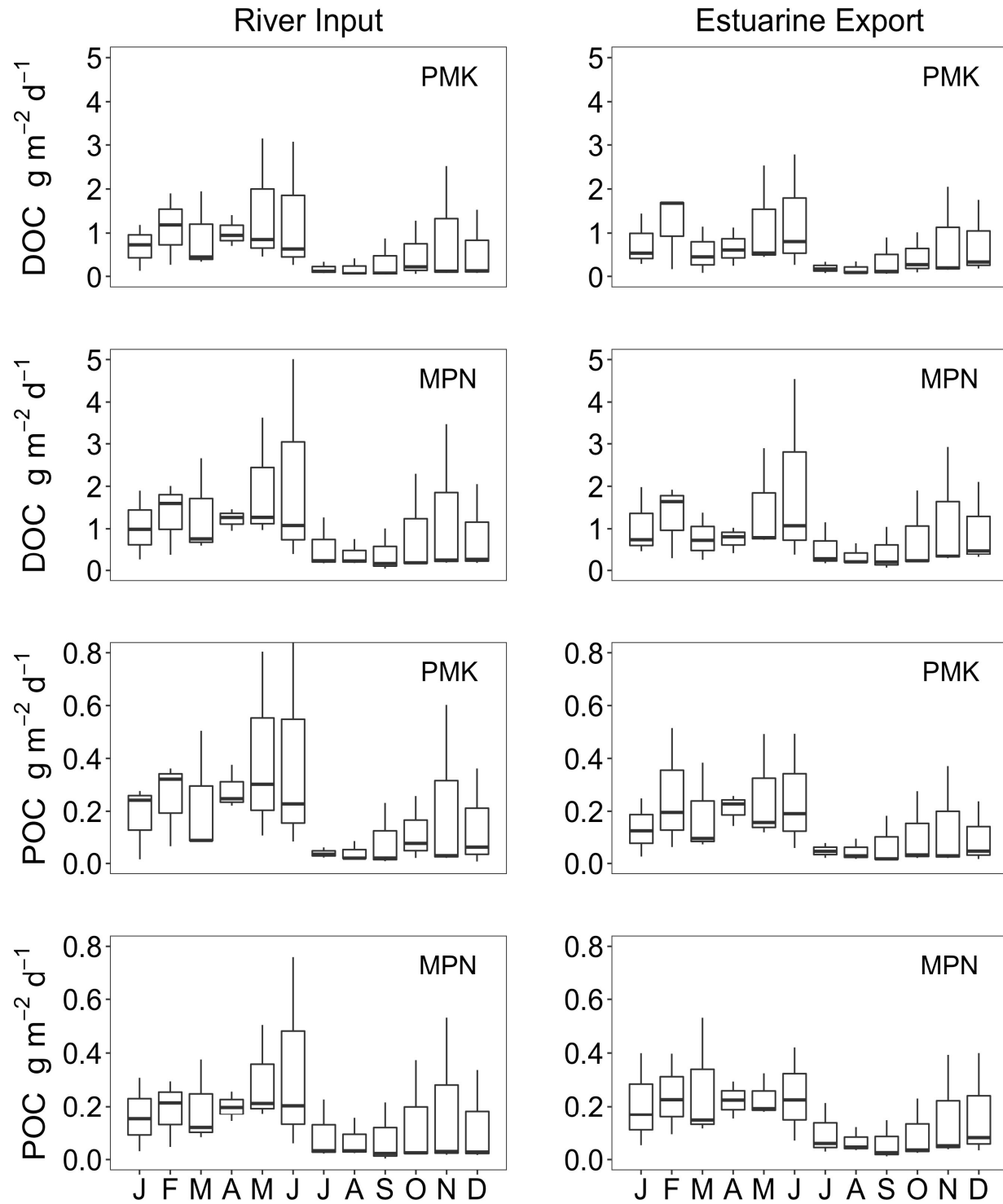
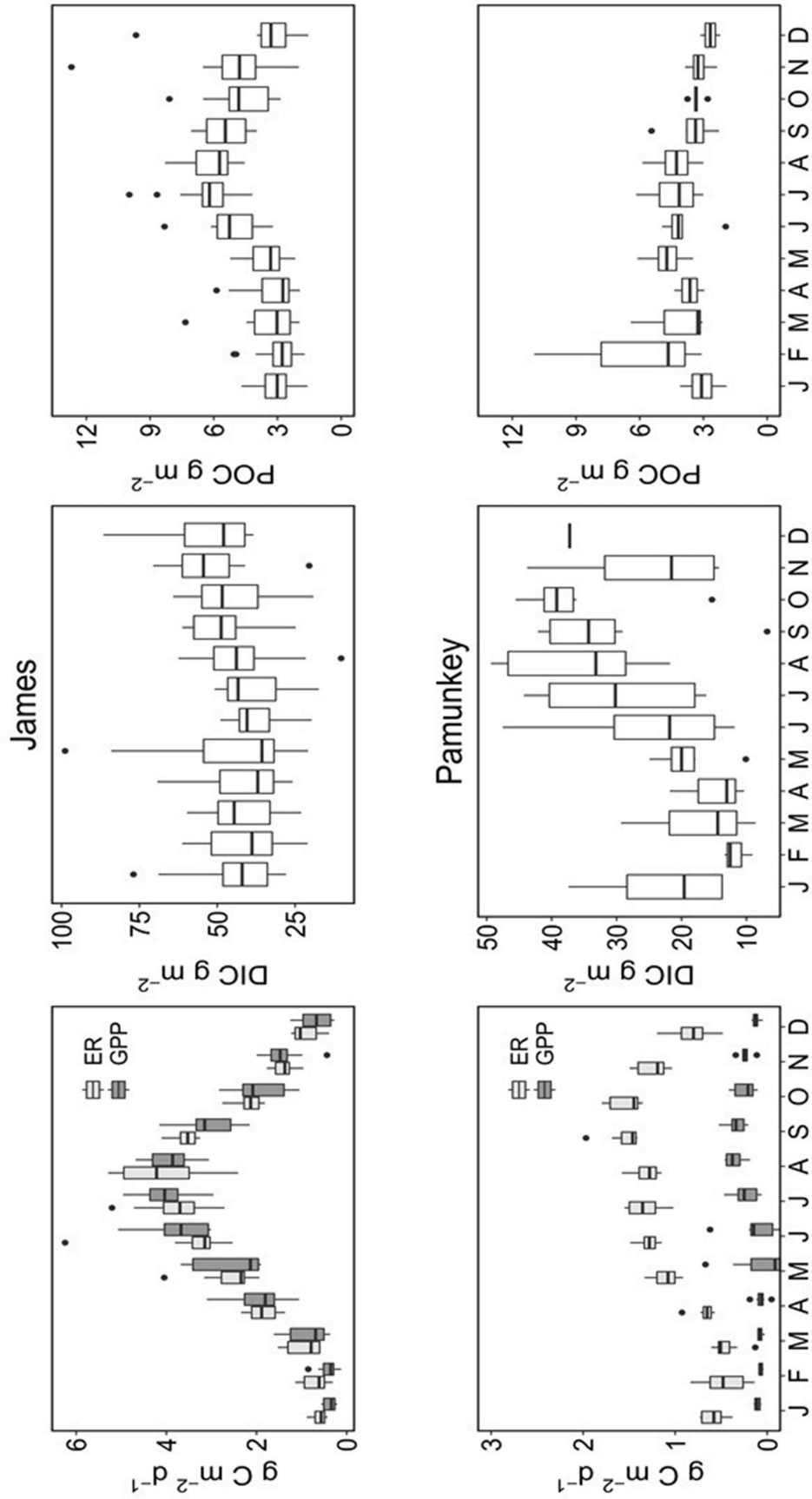


Figure 10. Seasonal variation in ecosystem metabolism (GPP and ER) in comparison to DIC and POC concentrations in the James and Pamunkey estuaries.



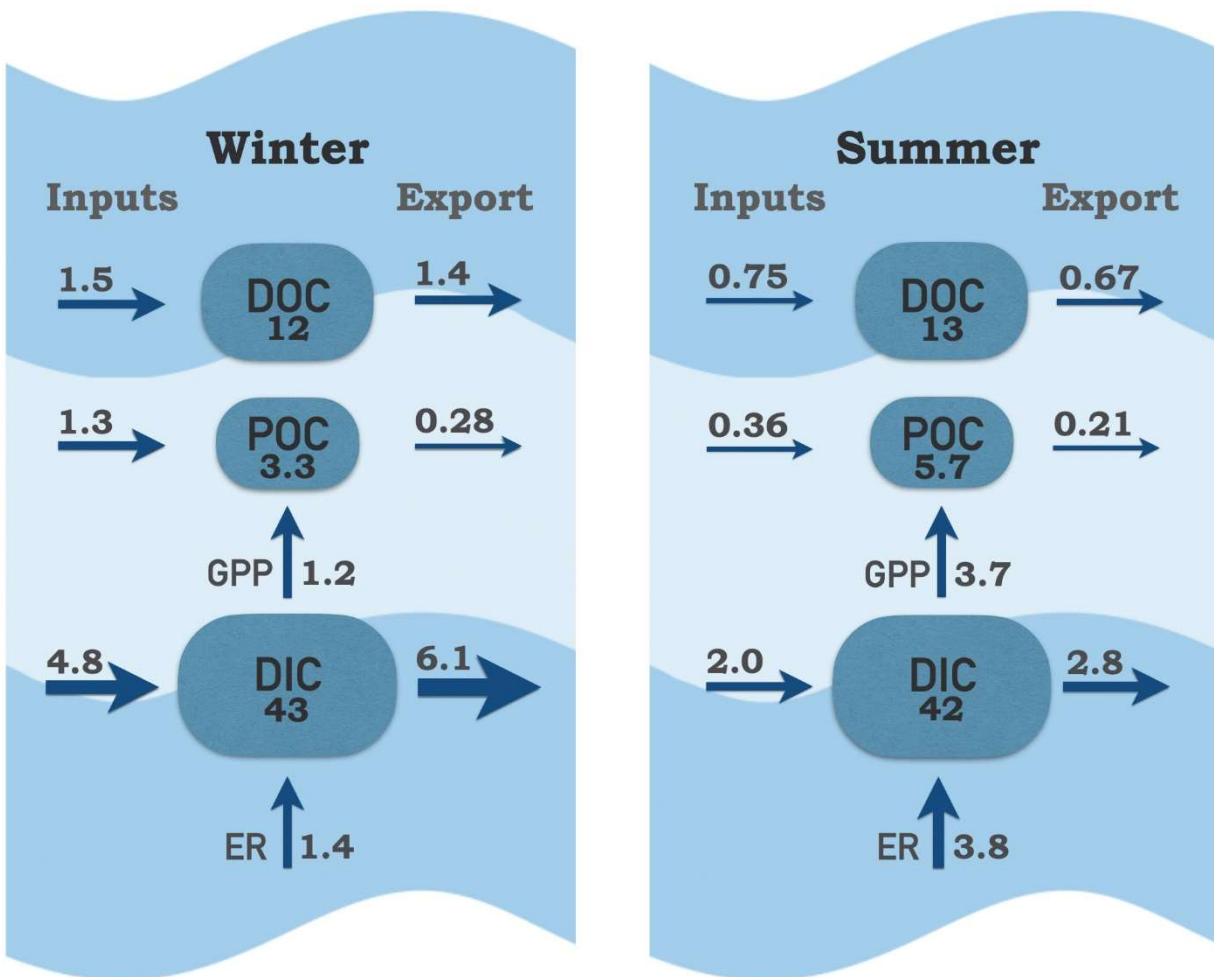


Figure 11. Carbon pools and fluxes within the tidal fresh segment of the James Estuary during winter (Jan-May) and summer (June-Sept). Inputs include riverine, local tributary and point source contributions; exports include tidal exchange and atmospheric losses of CO_2 . Carbon pools (boxes) are g C m^{-2} ; fluxes (arrows) are $\text{g C m}^{-2} \text{d}^{-1}$.